

1 **Hidden Impacts of Plastic Pollution on Coral Embryos**

2 **Sarah Tanja¹, Steven Roberts¹, Francesco Saliu², Stephan Salipante³,**
3 **Jacqueline L. Padilla-Gamiño¹**

4 ¹School of Aquatic & Fishery Sciences, University of Washington, Seattle, WA, United States,

5 ²Department of Earth and Environmental Sciences, University of Milano-Bicocca, Milan, Italy,

6 ³Department of Laboratory Medicine & Pathology, University of Washington, Seattle, WA, United States,

Corresponding author: Sarah Tanja, stanja@uw.edu

Abstract

Ocean plastic pollution releases chemical compounds as materials degrade. Polyvinyl Chloride (PVC) in particular contains high levels of endocrine-disrupting additives that are ubiquitously released into coastal environments as leachate. Despite this, the impacts of PVC leachate on marine life remain poorly understood. We investigated the ecotoxicological responses of three levels of PVC leachate (0.01 mg/L, 0.1 mg/L, 1 mg/L) during the first 14 hours post fertilization (hpf) of embryonic development in the coral *Montipora capitata*. PVC leachate did not affect embryo survival or the rate of morphological abnormality; however, we did detect subtle changes in developmental timing. Furthermore, RNAseq analysis identified 130 differentially expressed genes (DEGs) responsive to PVC leachate treatments. Gene expression responses to leachate exposure were strongest at low (0.01 mg/L) and moderate (0.1 mg/L) levels, and during the earliest developmental stage (cleavage, 4 hpf), indicating a non-monotonic response pattern and suggesting sublethal effects of low-dose PVC leachate exposure in developing *Montipora capitata* embryos. Additionally, analysis of 16S rRNA gene sequences (V4 region) revealed 9 bacterial taxa and 17 predicted microbial functional pathways responsive to PVC leachate, with differences in abundance and/or prevalence compared to controls. Our findings indicate that current environmental levels of PVC pollution may already subtly influence gene expression and early microbiome assembly in coral embryos as early as 4 hours post-fertilization, providing new insights into the sublethal, mechanistic impacts of plastic-derived chemicals.

Plain Language Summary

Plastic pollution in the ocean releases chemicals as materials break down. One common plastic, polyvinyl chloride (PVC), contains additives that can interfere with hormones and are released into seawater. However, we still know little about how these chemicals affect marine life. We studied how PVC leachate affected early embryos of the coral *Montipora capitata* during the first 14 hours after fertilization. Embryos were exposed to three levels of PVC leachate (0.01, 0.1, and 1 mg/L). PVC leachate did not reduce embryo survival or increase obvious deformities, but it did cause small shifts in developmental timing. We also examined changes inside the embryos using RNA sequencing and found 130 genes whose activity changed after exposure. The strongest responses occurred at the low and moderate levels, especially during the earliest stage of development (4 hours after fertilization). This suggests that even low levels of PVC chemicals can affect coral embryos in subtle ways. We also found changes in the bacterial communities associated with embryos, with 9 bacterial types differing across treatments. Overall, our results suggest that environmental levels of PVC pollution may already be affecting coral embryos by altering gene activity and early microbiome development only hours after fertilization. These hidden effects could have important consequences for coral health and reef resilience.

1 Introduction

Petroleum-derived plastic pollution is a rapidly escalating environmental concern (Stubbins et al., 2021). Global plastic production has doubled over the last decade, reaching an estimated 400 million tons in 2026. Of this, approximately 8-13 million tons of mismanaged plastic waste end up in the oceans annually, adding to an estimated 200 million tons already present in marine environments (Jambeck et al., 2015). Plastic pollution is increasingly concentrated in marine biodiversity hotspots, where major inputs from coastal regions in the Indo-Pacific overlap with coral reef ecosystems of exceptional ecological value, including the Coral Triangle (Figure 1). Ocean currents also transport and accumulate this debris in large offshore systems such as the Great Pacific Garbage Patch, highlighting how regional and coastal plastic pollution can be both a local and a global issue.

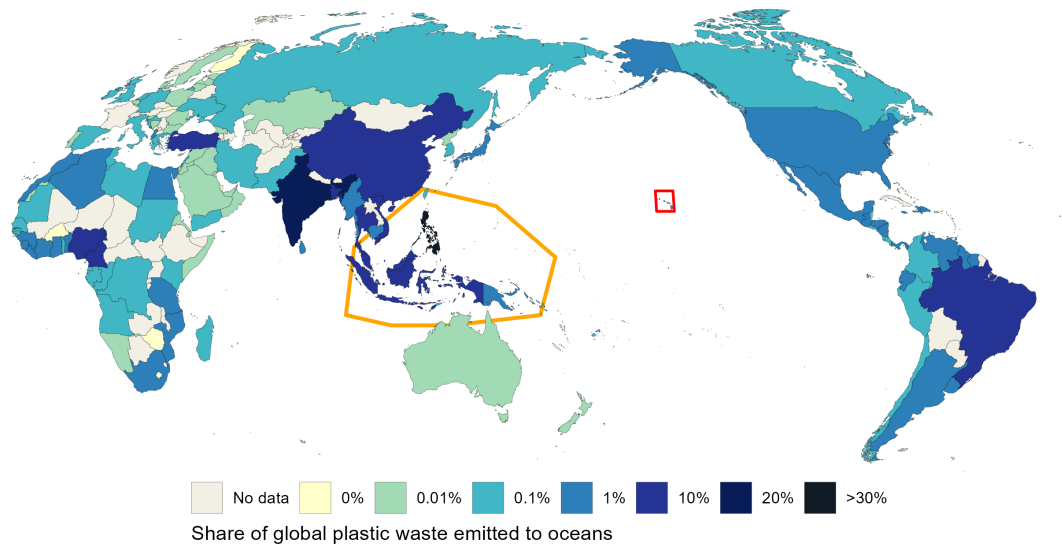


Figure 1: Share of global plastic waste emitted to the ocean, 2019 Annual estimate of plastic emissions. A country's total does not include waste that is exported overseas, which may be at higher risk of entering the ocean. Data sourced from (Meijer et al., 2021) - processed by Our World in Data (Ritchie, 2026). Locations of the Coral Triangle and the Hawaiian Islands indicated by outline.

58 Once in the ocean, plastics are exposed to UV radiation and mechanical weathering
 59 causing them to become brittle and fragment into microplastics (plastics < 5 mm)
 60 and nanoplastics (plastics <1 mm) (MacLeod et al., 2021). As plastics break down
 61 physically, they also undergo chemical degradation, releasing chemical additives
 62 and breakdown products directly into coastal waters as leachate (Hahladakis et al.,
 63 2018). These leachates originate from multiple sources, including landfills, sewage, and
 64 nonpoint-source runoff, and ultimately concentrate in urban coastal zones. Whether
 65 in marine or terrestrial environments, plastic debris can release more than 10,000
 66 chemical compounds. There is growing public awareness and concern over the impacts
 67 of plastic-derived leachate on human and environmental health.

68 Plastic leachate is a complex chemical mixture containing additives and degradation
 69 byproducts, such as UV stabilizers, colorants, plasticizers, bisphenol A (BPA), and
 70 per- and polyfluoroalkyl substances (PFAS) (Rochman et al., 2019). Among these,
 71 plasticizers (especially phthalates or phthalate acid esters (PAEs) used to enhance
 72 plastic flexibility), are the most abundant, accounting for up to 70% of the mass
 73 of PVC products. Phthalates are endocrine-disrupting chemicals (EDCs) that can
 74 mimic or interfere with hormonal signaling pathways that regulate developmental,
 75 reproductive, and immune function in both humans and wildlife (Maqbool et al.,
 76 2016). These additives are increasing in the marine environment alongside overall
 77 plastic pollution.

78 Early life stages in marine invertebrates (embryos and larvae) are often especially
 79 vulnerable to pollution (Richmond et al., 2018). Coral embryos are lipid-rich, and
 80 may be particularly susceptible to phthalates and other EDCs which are lipophilic.
 81 While endocrine signaling in cnidarians is not fully understood, endocrine hormones
 82 are known to play important roles in coral spawning timing, and embryonic cellular
 83 development (A. M. Tarrant et al., 2004; A. M. Tarrant, 2005; Ann M. Tarrant,

2007). There is potential for plastic-derived leachate endocrine-like disruption, and if coral sexual reproduction and recruitment is negatively impacted, whole coral reef ecosystems could be degraded over time (Richmond, 1997).

Relatively few studies have investigated the impacts of plastic-derived leachate on marine invertebrates. Studies that have been conducted primarily measure effects on fertilization, survival, development, larval motility, settlement, and metamorphosis. Phthalates and leachates from weathered polyvinyl chloride (PVC) affect larvae in the sea urchins *Paracentrotus lividus* (Gambardella et al., 2024; Jimenez-Guri et al., 2023; Rendell-Bhatti et al., 2021) and *Strongylocentrotus purpuratus* (Paganos et al., 2023). Embryonic development of the brown mussel, *Perna perna*, is sensitive to microplastic leachate (Gambardella et al., 2024). Even leachate from bioplastics contain additives that reduce egg fertilization, larval motility, and survival during the early development of the mussel *Mytilus galloprovincialis* (Capolupo et al., 2023). In the stony coral *Stylophora pistillata*, high exposure levels of dimethyl phthalate (DMP, 100 ug/L) reduced larval settlement, while exposure to environmentally relevant levels of plastic additive (1 ug/L of 4-nonylphenol 4-NP) reduced settlement of the soft coral *Rhytisma fulvum* (Vered & Shenkar, 2022). (Berry et al., 2019) found limited effects of weathered polypropylene on fertilization of the broadcast spawning coral, *Acropora tenuis*, but no significant effects on embryo development and larval settlement. Wilkins et al. (2024) found no reduced fertilization rates in *Montipora capitata* exposed to microplastics and leachates from commercially sources virgin PP, HDPE, and LDPE microspheres. (Wilkins & Richmond, 2025) found delayed or cumulative effects of reduced planulae survival and settlement in *Montipora capitata* and *Porites* corals exposed to virgin LDPE and HDPE leachates - and HDPE promoted settlement.

Together these studies indicate that leachate may be more toxic than physical particles, and weathered plastics are more toxic than virgin plastics. They also highlight the complexity of studying plastic-derived leachate and how our understanding of the current impacts of plastic leachate on marine organisms remains limited for several reasons. Plastic leachates are complex mixtures of thousands of additives whose composition varies with polymer type, age, and weathering state, making it difficult to standardize exposure treatments (Gunaalan et al., 2020). Many leachate compounds occur at very low environmental concentrations (ng-ug/L range), and their detection and quantification require highly sensitive analytical techniques, specialized expertise, and advanced infrastructure (Saliu et al., 2020). In addition, many past experimental studies still rely on high, acute exposure concentrations, which limit physiological interpretation in an environmentally relevant context (Weis & Palmquist, 2021). Finally, integrative physiological studies remain scarce, with most research focusing on survival, growth, or gross developmental endpoints rather than mechanistic responses such as gene expression or microbiome dynamics.

In this study, we chose to focus on exploring the potential for endocrine-like disruption and non-linear responses in early life history stages of coral. We chose PVC plastic because it has the highest phthalate content. We examined how PVC microplastic leachate impacts the development, microbiome, and transcriptomic signatures of embryos of the coral *Montipora capitata*. Coral reefs are one of the most valuable ecosystems on the planet; despite covering less than 1% of the oceans, they support at least 25% of all marine species (Reaka-Kudla, 1997). Reef-building corals provide global services estimated to be worth US\$2.7 trillion per year by protecting coasts from storm surge and wave erosion, supporting tourism and fisheries, and contributing to medicinal compound discovery (Souter et al., 2020). However, coral reefs are already in decline with global cover reduced by around 50% since the 1950s, and vulnerable to increasing coastal marine plastic pollution (Eddy et al., 2018, 2021; Oppen et al., 2017). Plastic pollution is ubiquitous across coral reef ecosystems globally (Pinheiro et al., 2023) as they are located near major coastal

sources of plastic input and are influenced by the same oceanographic systems that transport and concentrate marine debris (Lamb et al., 2018). One study found that plastic debris correlated with higher rates of disease (Lamb et al., 2018), and another showed that poorer water quality, due to closer proximity to an urban center, reduced recovery after a heatwave-induced bleaching event (Claar et al., 2020).

M. capitata is a broadcast spawner that releases gametes into the water column during synchronous spawning events. Fertilization and embryonic development occur in the water column before larvae settle and undergo metamorphosis. Early life history stages can be particularly vulnerable to plastic leachates due to direct exposure to surrounding seawater and their high sensitivity during critical periods of cellular differentiation (Lynch et al., 2022; Zhang et al., 2021).

Given that PVC leachates contain endocrine disrupting chemicals with potential to induce low-dose effects at environmentally relevant concentrations, we hypothesize that PVC leachate exposure would produce low-dose effects across organismal, transcriptomic, and microbiome responses. Specifically, we predicted that PVC leachate exposure would:

H_1 Reduce embryo survival and impair normal development

H_2 Alter gene expression in pathways required for early embryonic development

H_3 Disrupt the microbiome community and microbial function

This study provides insight into how plastic-derived chemical pollution may affect coral early life stages, a critical but under-explored phase of reef resilience and recovery.

2 Methods

2.1 Gamete collection and ecotoxicity assay exposure

The rice coral, *Montipora capitata*, is an ecologically important reef builder, and is a hermaphroditic synchronous split-spawner that releases buoyant egg-sperm bundles during the summer months (Padilla-Gamiño & Gates, 2012). In our study, we collected coral colonies on June 30th, 2024 from Kāne ohe Bay, on the east shore of Oahu, Hawaii. Kāne ohe Bay is a 60 km² embayment with several riverine inputs, numerous fringing and patch reefs, and a large barrier coral reef rimming it. Under the State of Hawai'i Division of Aquatic Resources Special Activities Permit 2024-35, we collected 20 genetically distinct *M. capitata* coral colonies (each approximately 30 cm in diameter) via snorkel from Patch Reef #1 at 21.431619°N, 157.787127°W.

Immediately after collection, the coral colonies were carefully transported to the Hawai'i Institute of Marine Biology (HIMB), placed in two large 650 L holding tanks with flow-through seawater, and allowed to acclimate for 5 days prior to the spawning event during the new moon (Padilla-Gamiño et al., 2011). Egg-sperm bundles of *Montipora capitata* were collected across three consecutive nights (5th, 6th, and 7th of July 2024, on the new moon and 2 days after). On each night prior to spawning (~19:00 HST), coral colonies were isolated in individual 12-quart (11.36 L) containers surrounded by a flow-through seawater bath to maintain stable ambient seawater temperatures (26.3 ± 0.3 °C). Sixteen out of the twenty parent colonies spawned over the three-day event (Figure 17). We collected egg-sperm bundles from spawning colonies using transfer pipettes and deposited them into labeled 50 mL Falcon tubes containing 30 mL of 0.22 μ m-filtered seawater (FSW). In the 1-hour window after egg-sperm bundle release and before bundle breakup, sperm release, and egg hydration, we performed controlled fertilizations by combining one intact bundle from each of two genetically distinct colonies in a bundle-bundle cross (Figure 2). Only intact bundles were used. Crosses were conducted in 20 mL scintillation vials containing 20 mL of either 0.22 μ m filtered seawater (control) or one of the three PVC leachate treatments. Fertilized bundles were incubated on a laboratory bench in the dark at

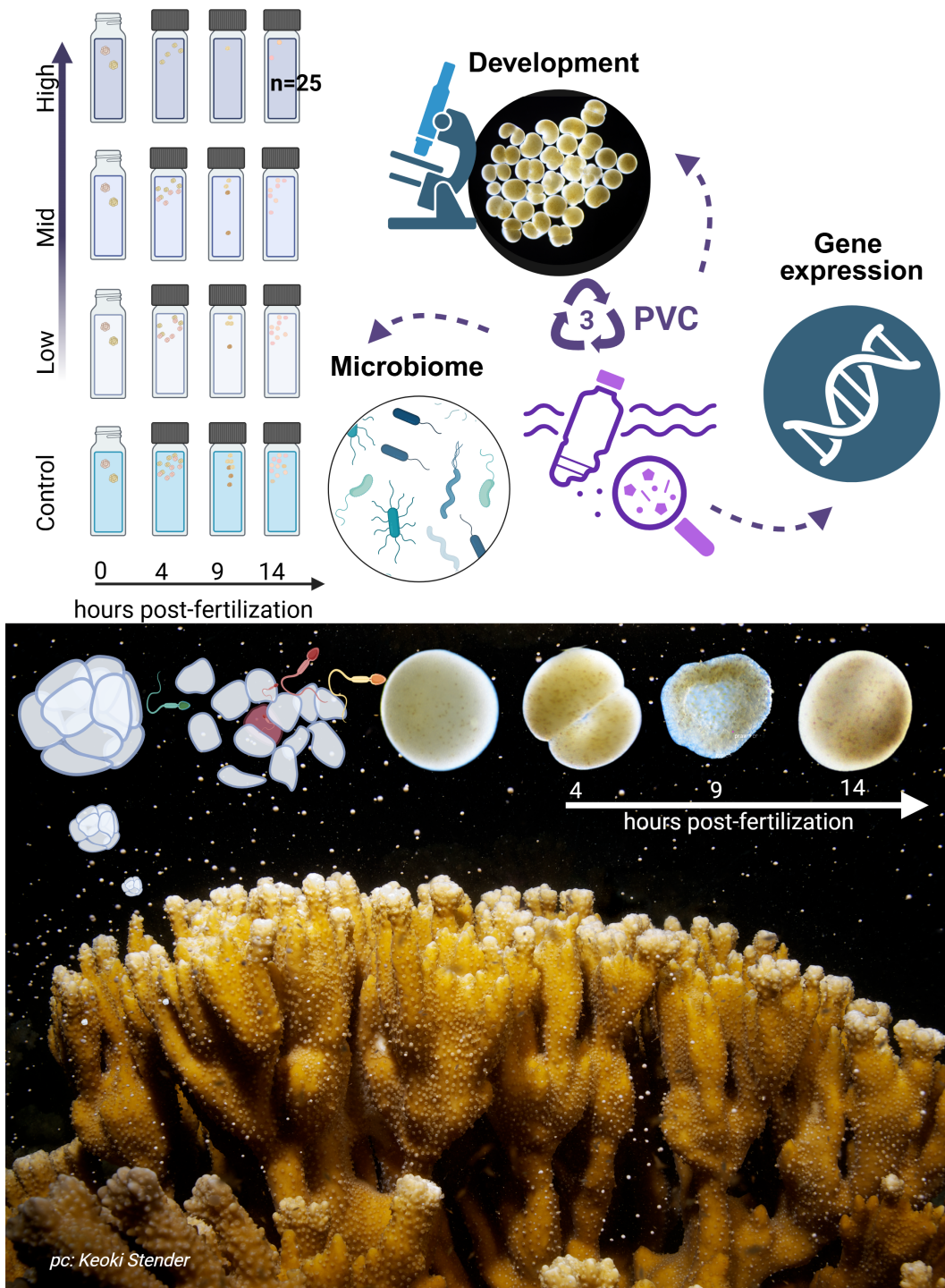


Figure 2: Experimental overview of *Montipora capitata* early life-stage exposure to PVC leachate. Schematic showing the reproductive biology and experimental design used to obtain coral embryos and assess the effects of plastic-derived leachates during early development.

189 26.8 ± 0.3°C for either 4, 9, or 14 hours post-fertilization (hpf). In *Montipora capitata*,
190 these time points correspond to key developmental stages: 4 hpf (initial cleavage
191 Figure 3 B-D), 9 hpf (prawnchick stage Figure 3 K-N), and 14 hpf (early gastrulation
192 Figure 3 O,P). The experiment included 4 PVC leachate levels and 3 developmental
193 stages, and resulted in 300 individual bundle-bundle crosses (Figure 2). A subset
194 of 120 crosses (40 per stage) was fixed in 1.5 mL snap-cap micro-centrifuge tubes
195 with 1 mL of 4% Z-fix (Anatech Ltd.) for assessment of survival, morphology, and
196 developmental progression via microscopy. The remaining 180 crosses (60 per stage)
197 were preserved in 500 L of DNA/RNA Shield™ (Zymo Research, USA) and stored
198 at -80°C for subsequent DNA and RNA extraction to investigate microbial community
199 composition and gene expression responses.

200 **2.2 PVC leachate preparation, dilution, and analysis**

201 PVC microplastics were obtained following the procedure described by Isa et al.
202 (2024). Briefly, PVC granulates 500 µm were obtained by grinding PVC pellets,
203 and polymer identity was confirmed by FTIR analysis (see supplementary material
204 X). The material was then subjected to artificial weathering in a QUV accelerated
205 weathering tester (Q-LAB, Saarbrücken, Germany) using UV lamps at 340 nm, with
206 0,76 W m⁻² nm⁻¹. The aging test was conducted at 65°C for a total time of 460 h.
207 The total UV dose administered (measured by a bolometer) was 170 MJ/m². This
208 dose roughly corresponds to 10 months of outdoor exposure at 31°N latitude (Isa et
209 al., 2025) to simulate photo-degradation processes experienced by plastic debris in the
210 marine environment.

211 We prepared the PVC leachate by adding 250 mg of UV-weathered PVC microplastics
212 to 250 mL of 0.22 µm-filtered seawater (FSW) collected from Kāne ohe Bay in a 400
213 mL Erlenmeyer flask. The mixture was shaken in a flask at 90 rpm in the dark for
214 seven days. Following incubation, microplastics were removed by filtration using a
215 0.22 µm cellulose fiber filter, leaving a concentrated PVC leachate nominally equivalent
216 to 1 g/L of PVC microplastics in seawater. This stock solution was then serially
217 diluted with 0.22 µm FSW to produce the experimental treatments: 0.01 mg/L (low),
218 0.1 mg/L (moderate), and 1 mg/L (high) PVC leachate. Stock solution leachates were
219 chemically characterized by GC-MS (full scan mode) and LC-MS/MS (MRM, multiple
220 reaction monitoring mode) following the method of Saliu et al. (2020). These analyses
221 indicated that the leachate contained phthalates at approximately 10% of the original
222 PVC microplastic mass concentration. So while our treatments are characterized by
223 the mass of PVC microplastic used to generate the leachate, the concentrations of
224 chemical additives, such as phthalates, are estimated to be ~1 µg/L (low), ~10 µg/L
225 (moderate), and ~100 µg/L (high).

226 Importantly, the selected exposure levels span reported environmental concentrations
227 of phthalates in coastal surface waters, which range from 0 (limit of detection, LOD)
228 to 168 µg/L (Hermabessiere et al., 2022; Law et al., 1991; Mathieu & Bednarek, 2022;
229 Net et al., 2015; Paluselli et al., 2018), addressing a common limitation of previous
230 studies, which lack environmentally relevant exposure levels (Weis & Palmquist,
231 2021). Our PVC leachate treatments reflect the full chemical mixture derived from
232 UV-weathered PVC microplastics, rather than exposure to individual additives. Due
233 to analytical limitations, exposure levels are reported as nominal values, consistent
234 with established practices in leachate toxicity studies (Tetu et al., 2019; Vered &
235 Shenkar, 2022).

236 **2.3 Imaging and annotation**

237 Embryos preserved in 4% Z-Fix (aqueous zinc-buffered formalin diluted in 0.22 µm
238 FSW) were permanently mounted on microscope slides using glycerol as a mounting
239 medium. Imaging was conducted with a Nikon DS-Fi 3 camera attached to a Nikon
240 Eclipse Ni-U manual microscope, and a composite image for each slide was generated
241 through manual stitching. Images were analyzed using NIS-Elements BR software

242 (version 5.02.01) to quantify the total number of embryos per treatment vial. We
 243 determined developmental stage reached of each embryo (egg, cleavage, morula,
 244 prawnchip, or early gastrula), and noted any morphological deformities or uncertainty
 245 due to fragmentation (typical, uncertain/torn, malformed). We chose to annotate
 246 the morphology of a torn embryo as uncertain, because coral embryos are known
 247 to continue developing even after fragmentation in early embryonic development
 248 (Heyward & Negri, 2012). At 4 hours post-fertilization (hpf), samples are expected to
 249 reach the initial cleavage stage, characterized by the division of the fertilized oocyte
 250 into two blastomeres (Okubo et al., 2013). At 9 hpf, embryos are expected to reach
 251 the prawnchip phase, and at 14 hpf, coral embryos are expected to reach the early
 252 gastrula stage (E. E. Chille et al., 2022; Okubo et al., 2013). Examples of normally
 253 developed *M. capitata* embryos are shown in Figure 3. Our annotated images are
 254 available at <https://github.com/sarahtanja/coral-embryo-scope/tree/main/scope-images>.
 255

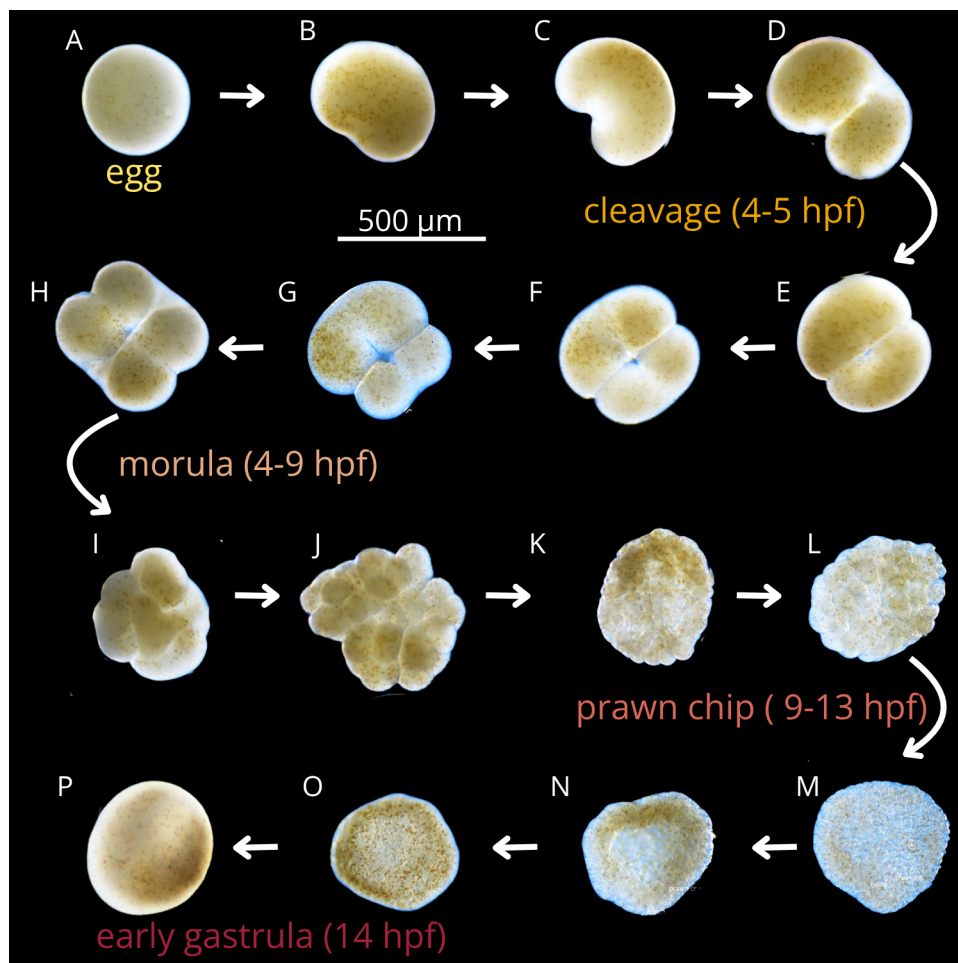


Figure 3: Developmental progression of *Montipora capitata* embryo from egg to early gastrula during the first 14 hours post fertilization.

256 2.4 Quantifying relative survival

257 At the beginning of the experiment, each vial contained two gamete bundles, corre-
 258 sponding to an average starting total of $\sim 30 \pm 6.4$ eggs, based on previously reported
 259 estimates of 8-23 eggs per bundle (mean=15, SD= ± 5.1 , SE= ± 0.3 , [Padilla-Gamiño

et al. (2011); Padilla-Gamiño & Gates (2012);]). Viable embryos per vial at each time point were used as the response variable. Embryos classified as ‘typical’ or ‘torn’ were considered viable, while ‘malformed’ embryos were excluded from viable embryo counts. Torn embryos were included because early coral embryos can continue developing after fragmentation due to cellular totipotency (Heyward & Negri, 2012). Eggs at 4 hpf were considered viable unless malformed; by 9 and 14 hpf any remaining eggs that were unfertilized or not developmentally progressing were classified as non-viable. Raw counts were imported and pre-processed in R (v4.5.1) using the tidyverse packages (Wickham et al., 2019). Treatment and time were coded as categorical factors and were explicitly ordered. Survival was analyzed as the counts of viable embryos at each time point. Distributions of viable embryo counts were visualized using boxplots with beeswarm overlays, showing individual vial-level observations across treatment \times time combination (Figure 4). A two-way analysis of variance (ANOVA) was used to test the effects of treatment, developmental time (hpf), and their interaction on viable embryo counts. Model assumptions were evaluated using residual Q-Q plots, the Shapiro–Wilk test for normality, and Levene’s test for homogeneity of variances. All statistical tests were two-tailed with $\alpha = 0.05$. Data analysis for embryo survival is available at https://github.com/sarahtanja/coral-embryo-scope/blob/main/code/03_survival.md.

2.5 Quantifying developmental timing

To assess if PVC leachate altered early embryonic developmental timing, we quantified the number of embryos in five developmental stages—egg, cleavage, morula, prawnchips, and early gastrula—for each sample. Because these data are multivariate counts and exhibited overdispersion (variance = 45.1, mean = 3.58), we used a multivariate generalized linear model (GLM) implemented in the mvabund package (mvabund_4.2.1, function manyglm; Wang et al. (2012)). Counts of developmental stages were modeled simultaneously as a multivariate response ($Y \sim \text{treatment} * \text{hpf}$) using a negative binomial error distribution, with the log of the embryo counts in each sample as an offset term. The offset term ensures that the model captures shifts in the ratios of stages rather than in absolute counts for each developmental stage. The full dataset was analyzed as a single multivariate response matrix, allowing us to detect both overall shifts in development and stage-specific responses. Model significance was assessed using PIT-trap resampling with 999 iterations, which provides robust p-value estimation under non-normal residual structure. We report multivariate test statistics (evaluating changes in developmental stage across treatments and time) and univariate tests for each stage. Significance of main effects and interaction terms was assessed using Analysis of Deviance (Type I tests). All analyses were performed in R (v4.5.1) with $\alpha = 0.05$. The R code used for the developmental timing analysis is available at https://github.com/sarahtanja/coral-embryo-scope/blob/main/code/04_timing.md.

2.6 Quantifying morphological abnormality

Similarly to developmental timing, we analyzed morphological status using a multivariate generalized linear model (GLM). We tested whether PVC leachate altered the counts of embryos classified as typical, uncertain (torn), or malformed across developmental time. For each sample, embryo counts were grouped into these three categories. Because the data were overdispersed (variance = 76.5, mean = 5.97), we specified a negative binomial error distribution. To account for changes in embryo counts due to survival, we included the log of the embryo counts in each sample as an offset term. The multivariate response matrix (Y) included counts of typical, uncertain (torn), and malformed embryos. The model tested the effects of treatment, developmental time, and their interaction ($Y \sim \text{treatment} * \text{hpf}$). The R code and our analysis for morphological abnormality are available at https://github.com/sarahtanja/coral-embryo-scope/blob/main/code/05_abnormality.md.

2.7 DNA/RNA extractions and quantification

At each developmental endpoint (4, 9 and 14 hpf), coral embryos were transferred from exposure vials to 2 mL microcentrifuge tubes, preserved in DNA/RNA Shield™ (Zymo Research, USA), and stored at -80°C. DNA and RNA were extracted simultaneously from the same pooled samples using the Quick-DNA/RNA™ Miniprep Plus Kit (Zymo Research, USA). Samples of embryos in DNA/RNA Shield™ were thawed to room temperature and pooled with up to three coral colony crosses from the same treatment group to achieve sufficient DNA/RNA yield (pooled sample structure is shown in Figure 17). Samples were pooled in ZR BashingBead Lysis Tubes™ (0.1 and 0.5 mm) (Zymo Research, USA) and homogenized for 10 minutes using a Morterex. Extraction and purification steps followed the manufacturer’s cell preparation protocol, but skipped the proteinase-K digestion step. Purified total RNA was quantified using a Qubit-4 Fluorometer with the RNA High Sensitivity Assay Kit (ThermoFisher, USA) and shipped on dry ice to Azenta Life Sciences for library preparation with Poly(A) selection. DNA was similarly quantified using the dsDNA Broad Range (BR) Assay Kit (ThermoFisher, USA) according to the manufacturer’s protocol. This resulted in 63 pooled samples from which both DNA and RNA were extracted. These samples are paired, i.e. DNA and RNA was extracted from the same embryos for each of the 63 pooled samples. Each pooled sample represents genetic variation from up to six parent colonies (Figure 17).

2.8 Transcriptomics (RNA library prep, sequencing, processing, and analysis)

2.8.1 RNA library preparation, and sequencing

Our 63 pooled samples of total purified RNA were processed for library preparation and sequencing (Azenta Life Sciences). Libraries were prepared using Poly(A) selection to target eukaryotic mRNA, with a sequencing depth of 20 million paired-end reads per sample. Sequencing was performed on an Illumina NovaSeq X+ platform (x150bp). Raw paired-end reads (FASTQ format) were submitted to the National Center for Biotechnology Information (NCBI) Sequence Read Archive (SRA) under BioProject accession number PRJNA1177827.

2.8.2 Quality checks, alignment, and gene count matrix generation

Raw paired-end FASTQ files were checked for quality with FastQC (v0.12.1) and summarized using MultiQC (v1.14) (Ewels et al., 2016). Adapter sequences were trimmed, and sequences were pre-processed with fastp (v0.23.2) (Chen, 2023) using automatic adapter detection for paired-end data, a phred quality score threshold of 30, removal of polyX tails 6 bp, and fixed trimming of 10 bp from the 5 end of both forward and reverse reads. Trimmed reads were aligned to the *M. capitata* reference genome (Hiv3; Rutgers Coral Genome Project (Stephens et al., 2022)) using HISAT2 (v2.2.1) (D. Kim et al., 2019) with splice-aware alignment. Exon coordinates and splice junctions were extracted from the genome annotation file (GTF) with HISAT2 helper scripts provided during alignment to improve mapping across intron–exon boundaries. The resulting SAM files were converted to sorted and indexed BAM files using SAMtools (v1.12) (Danecsek et al., 2021). Transcript assembly and abundance estimation were performed with StringTie (v2.2.1) (Pertea et al., 2015), guided by the reference annotation (GFF3). A gene count matrix (genes x samples) was generated using the StringTie helper script prepDE.py3, enabling downstream differential expression analysis. The quality-assurance, quality-check (QAQC) and alignment R code can be viewed at <https://github.com/sarahtanja/coral-embryo-RNAseq/tree/main/code>.

2.8.3 Differential gene expression analysis with DESeq2

Raw gene counts were imported into R (v4.2.3) along with sample metadata. Genes with fewer than 10 counts in at least 85% of samples were removed prior to analysis. Count data were normalized using DESeq2 (v1.38.3) (Love et al., 2014), with

size factors estimated and variance-stabilizing transformation (VST) applied for downstream visualization. Principal component analysis (PCA) was performed on the 500 most variable genes to assess global sample structure and identify potential outliers (Figure 7 A). Outlier samples were flagged by visual inspection and Z-score thresholding (>3 standard deviations along PC1 or PC2) and subsequently removed. Two samples were excluded due to poor alignment in HISAT2 (131415L4 0.2%, 789C4 8.9%; MultiQC Bowtie2/Hisat2 report) and failure to cluster with other samples in the PCA plot. The remaining 61 samples had alignment rates ranging from 27.4% to 83.2%. Following outlier removal, gene filtering was repeated using the same filtering thresholds (retaining genes with ≥ 10 counts in at least 85% of samples). Sample-to-sample relationships were further analyzed using a z-score transformed heatmap with hierarchical clustering, with samples annotated by spawn night, leachate treatment and developmental stage (Figure 7 B).

Our DESeq2 (v1.38.3) (Love et al., 2014) model accounted for spawn night, stage, leachate, and the interaction between leachate and stage (\sim spawn_night + stage + leachate + stage:leachate). We chose to treat leachate and hours post fertilization as categorical factors to test for stage-specific differences without assuming a particular dose-response shape, since we were looking for non-linear response trends. To evaluate model structure, we conducted likelihood ratio tests (LRTs). We first analyzed the effect of spawn night by comparing the full model to a reduced model excluding spawn night. This analysis identified 3,551 genes ($\sim 29\%$) as significantly differentially expressed (Benjamini-Hochberg (BH) FDR-adjusted p -value < 0.05) indicating that spawn night contributes substantially to expression variability and represents a batch effect. Accordingly, spawn night was retained in the full model to control for the variability in gene expression due to the different nights on which our parent coral colonies spawned. We then used LRTs to confirm the inclusion of both leachate and the stage \times leachate interaction terms. Following these tests, Wald contrasts were performed to estimate \log_2 fold changes for pairwise contrasts, specifically assessing the effect of each leachate level at each developmental stage relative to the control, as well as the larger signal across developmental stages. Genes with false discovery rate (FDR) adjusted $p < 0.05$ were considered significantly differentially expressed in the LRT tests and Wald tests. We generated lists of DEGs responsive to leachate and to developmental progression.

We then grouped leachate-responsive DEGs and developmental progression DEGs by expression patterns. Because the number of leachate-responsive DEGs was relatively small ($n=130$) and pre-filtered, the scale-free topology criteria were not met; therefore expression patterns were summarized using trajectory-based clustering implemented in DEGreport v1.46.0, rather than co-expression network analysis. In contrast, the larger set of development-related DEGs (10,793 genes) was analyzed using weighted gene co-expression network analysis (WGCNA) with the WGCNA R package (v 1.73)(Langfelder & Horvath, 2008).

2.8.4 Gene ontology (GO) enrichment and slim characterization

We characterized the GO terms associated with all of our DEGs for each expression pattern subset. Significant genes identified in the DESeq2 analysis were functionally annotated and assessed for Gene Ontology (GO) enrichment. Protein-coding sequences from the *Montipora capitata* genome v3 (<http://cyanophora.rutgers.edu/montipora/>) were matched to EggNOG annotations, and gene lengths were extracted from the reference GFF3 file to account for length-dependent bias in RNA-seq detection. GO enrichment analysis was conducted using the R package goseq (v1.50.0) with Wallenius' distribution to correct for gene length bias (the increased detection power for longer genes) and restricting tests to biological process terms. A background universe of the filtered DESeq2 gene set (12,221 genes) was used. Significance was determined by Benjamini-Hochberg false discovery rate (FDR) correction, with GO terms retained at adjusted $p < 0.05$.

2.9 Microbiome (DNA library prep, sequencing, processing, and analysis)

2.9.1 DNA Amplification, Library Preparation, and Sequencing

Purified DNA for each of our 63 pooled samples was used directly for library preparation, without fragmentation or size selection. Amplicon libraries targeting the V3–V4 region of the 16S rRNA gene were generated following Illumina’s 16S Metagenomic Sequencing Library Preparation protocol (Illumina, Part no. 15044223 Rev. B) using primers 5 -CCTACGGGNGGCWGCAG-3 and 5 -GACTACHVGGGTATCTAATCC-3 (Klindworth et al. 2013). PCR amplification was performed according to the manufacturer’s guidelines. Libraries were sequenced at the University of Washington Microbiome Initiative (mim_c) on an Illumina NextSeq™ 2000 platform using the P1 600-cycle reagent kit. Raw paired-end reads were deposited in the NCBI Sequence Read Archive under BioProject accession number PRJNA1244351.

2.9.2 Amplicon Processing and Taxonomic Inference

All sequence pre-processing steps were performed in QIIME2 v2023.9 (Bolyen et al., 2019). Demultiplexed paired-end reads were trimmed with Cutadapt to remove primer sequences and then denoised with DADA2. QIIME2 was used to examine rarefaction curves, assess sequencing depth, infer amplicon sequence variants (ASVs), remove chimeras, and construct a feature table. Representative ASVs were taxonomically assigned using a pre-trained SILVA Naive Bayes classifier. ASVs classified as mitochondria, chloroplast, or unassigned were removed from the filtered feature table prior to downstream analyses.

2.10 Microbial community compositional data analysis

Data representing our 63 pooled samples coral embryo microbiome communities. Amplicon sequence variant (ASV) count data were analyzed following recommendations for microbiome sequence data, which are constrained by relative abundance and sequencing depth rather than absolute counts (Gloor et al., 2017). Analyses were conducted in R (v4.5.1) using the packages tidyverse, qiime2R, phyloseq, vegan, compositions, and zCompositions.

Because log-ratio transformations cannot accommodate zeros directly, zero counts were first replaced using count zero multiplicative replacement (cmultRepl, method = “CZM”). The zero-adjusted count matrix was then transformed using the centered log-ratio (CLR) transformation to map compositional data into Euclidean space suitable for standard multivariate analyses. The resulting CLR matrix contained 63 samples and 663 retained ASVs.

Between-sample dissimilarity (Beta diversity) was quantified using Aitchison distance, calculated as Euclidean distance on the CLR-transformed feature table. Principal components analysis (PCA) was then performed on the CLR-transformed matrix using the prcomp() function. To evaluate whether differences among groups reflected unequal within-group variability rather than centroid separation, homogeneity of multivariate dispersion was tested using betadisper(). Dispersion was evaluated separately for spawn night, leachate treatment, developmental stage, and the leachate × stage interaction.

Differences in microbial community composition across experimental factors (leachate*stage) were tested using permutational multivariate analysis of variance (PERMANOVA) implemented with adonis2() in the vegan package, with 999 permutations. To account for non-independence among samples collected on the same spawning night, permutations were constrained within spawn night using the strata argument. Terms were tested sequentially using the by = “terms” option. This approach allowed effects of leachate exposure and developmental timing to be evaluated while controlling for batch effects associated with the night of spawning.

2.10.1 Differential abundance & prevalence testing with *MaAsLin3*

Associations between microbial features and experimental variables were tested using *MaAsLin3* (Mallick et al., 2021) in R. Analyses were performed on taxonomic features collapsed to the genus level (Level 6). For both data types, features were retained if present in 5% of samples with relative abundance 0.1%. No additional normalization was applied, as inputs were proportion-normalized during preprocessing. Differential abundance and prevalence testing were performed using a generalized linear mixed-effects modeling framework implemented in *MaAsLin3* with the formula: abundance/prevalence \sim leachate * hpf + (1|spawn_night). Significance was determined by adjusted joint q-values < 0.1 , which were corrected for multiple testing with the Benjamini–Hochberg method for adjusting for false discovery rate.

2.10.2 Functional Prediction with *PICRUSt2*

Predicted functional profiles were inferred from 16S rRNA amplicon sequence variants (ASVs) using *PICRUSt2* (Douglas et al., 2020). A total of 547 *PICRUSt2* predicted *MetaCyc* pathways were included in downstream modeling. Differential abundance and prevalence testing of *MetaCyc* predicted pathways was conducted using *MaAsLin3* in R.

3 Results

3.1 H_1 : Survival and Development

3.1.1 Survival

Polyvinyl chloride (PVC) leachate did not change embryo survival during the first 14 hours post-fertilization (hpf) of embryonic development (Figure 4 a; treatment: $F_{3,96} = 0.523$, $p = 0.668$)(Table 2).

Time was the main factor affecting embryo survival. Mean counts of surviving embryos across replicate vials declined from 26.1 ± 4.4 SD at 4 hpf to 12.2 ± 7.4 SD at 9 hpf, and then remained relatively stable between 9 and 14 hpf (11.9 ± 5.7 SD) (hpf: $F_{2,96} = 64.04$, $p < 0.0001$). Survival was similar across all PVC leachate treatments (interaction: $F_{6,96} = 0.572$, $p = 0.752$), showing that neither exposure level nor exposure duration altered embryo survival trends. Model assumptions for our two-way ANOVA were met as residuals were normally distributed (Shapiro–Wilk normality test $W = 0.99$, $p = 0.69$) and variances were similar among groups (Levene’s $F_{\sim 11, 96} = 1.25$, $p = 0.26$).

3.1.2 Morphological abnormality

Morphological abnormality (embryos annotated as typical, uncertain/torn, or malformed) did not vary across PVC leachate treatments. The multivariate negative binomial model found that neither PVC leachate treatment (treatment: $Dev = 4.67$, $p = 0.607$) nor the relationship between PVC leachate treatment and developmental time (interaction: $Dev = 11.41$, $p = 0.770$) had any effect on morphological abnormality (Table 4).

However, we found developmental stage significantly impacted morphology status. Regardless of treatment, we found an increase in uncertain embryos ($Dev = 25.24$, $p = 0.002$) at the 9 hpf (prawnchip) stage, with a concurrent decrease in typical embryos ($Dev = 63.75$, $p = 0.001$)(Figure 4 C). Malformed embryos however did not vary significantly across developmental time ($Dev = 1.91$, $p = 0.366$) (Table 4).

Mean count summaries show that typical embryos were most abundant at 4 hpf across all treatments, then declined at 9 and 14 hpf, while uncertain embryos tended to peak at 9 hpf. Malformed embryos remained consistently low. Together, these results indicate that PVC leachate exposure had no significant effect on the counts of embryos classified as typical, uncertain/torn, or malformed (Figure 4 c). Overall the number of embryos found to be malformed were low compared to typically-formed embryos.

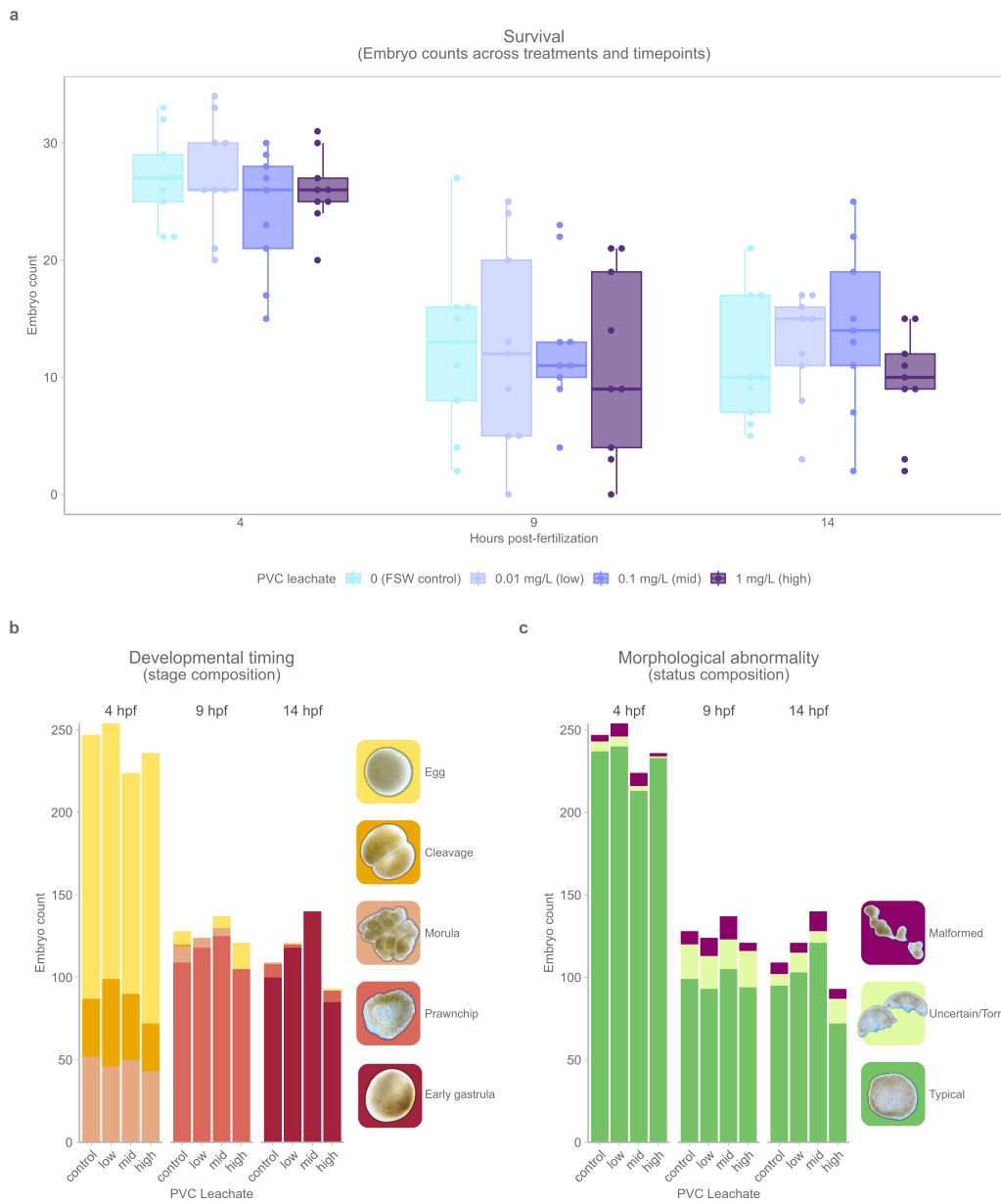


Figure 4: A. Total surviving embryo counts at 4, 9, and 14 hours post-fertilization (hpf) following exposure to increasing doses of PVC leachate; illustrating no differences in survival due to treatment B. Total embryo counts colored by embryonic stage (egg, cleavage, morula, prawnchip, early gastrula) for each treatment and time point; illustrating subtle shifts in stage composition in low and mid exposures at 9 and 14 hpf. C. Total embryo counts colored by morphology status (malformed, uncertain/torn, typical) for each treatment and time point; illustrating no differences in morphology due to PVC leachate treatment.

521 Anecdotaly, we observed that the secondary cell division (progressing from the 2-cell
 522 to the 4-cell stage) initiates at the center of the two blastomeres and extends outward
 523 (Figure 3 G). This contrasts with the primary cell division (initial cleavage) which
 524 begins at one pole of the fertilized egg and progresses across, which is evident in the
 525 heart-shaped embryos (Figure 3 C).

526 **3.1.3 Developmental timing**

527 We tested whether the mix of embryo developmental stages changed over time across
 528 PVC leachate treatments using a multivariate generalized linear model. As expected,
 529 embryo stage composition changed strongly with time (hpf: $Dev = 669.0$, $p < 2 \times 10^{-16}$
 530). At 4 hpf, most embryos were in the egg, cleavage, or morula stages. At 9 hpf, most
 531 embryos were in the prawnchip stage. By 14 hpf, the early gastrula stage dominated
 532 (Figure 4 B).

533 PVC leachate exposure alone did not cause an overall shift in the stage composition
 534 of embryos (treatment: $Dev = 1.2$, $p = 0.999$). However, treatment effects changed
 535 across time (interaction: $Dev = 48.1$, $p = 0.002$). When stages were examined sepa-
 536 rately, we found this pattern was driven mainly by differences in the prawnchip stage
 537 at 14 hpf (the interaction effect is localized to a specific prawnchip stage developmen-
 538 tal window), with weaker trends in the egg and morula stages. No treatment effects
 539 were detected in the cleavage or early gastrula stages.

540 Overall, these results suggest that PVC leachate did not broadly disrupt normal
 541 developmental timing, but it may have caused small, stage-specific changes, possibly
 542 speeding the morula to prawnchip transition at 9 hpf, and the prawnchip to early
 543 gastrula transition at 14 hpf under low and mid, but not high leachate (Figure 5, OR
 544 Figure 6).

545 **3.2 H_2 : Gene expression**

546 **3.2.1 Global expression**

547 Principal component analysis (PCA) was performed on variance-stabilized gene counts
 548 using the top 500 most variable genes as an exploratory tool to assess global patterns
 549 of variation. The first two principal components accounted for 72.4% of the total
 550 variance among samples and revealed strong clustering by early embryonic stage, with
 551 separation primarily along principal component 1 (PC1, 53.9% of global sample struc-
 552 ture variance) (Figure 7 A). Samples formed three distinct, non-overlapping clusters
 553 with minimal within-group dispersion, indicating that stage represents the dominant
 554 source of variance in the dataset. Principal component 2 (PC2, 18.5% of global
 555 sample structure variance) primarily captures the variation within groups, indicating
 556 that secondary sources of variation are present but do not override the dominant stage
 557 effect. Treatment-associated effects of PVC leachate were not readily apparent in the
 558 leading principal components. The pronounced stage-driven structure is consistent
 559 with large-scale transcriptional reprogramming during early embryogenesis (Figure 7
 560 B).

561 We followed visual PCA exploration with a permutational multivariate analysis of
 562 variance (PERMANOVA) to statistically test for treatment-associated effects. A
 563 PERMANOVA with 999 permutations was performed on the Euclidean distance
 564 matrix of transformed gene expression values to assess the effects of leachate level,
 565 developmental stage, and their interaction on global expression profiles while control-
 566 ling for variation among spawning nights (permutations were restricted or ‘stratified’
 567 within spawn night by setting the strata = spawn_night). The PERMANOVA
 568 identified developmental stage as the dominant driver of multivariate expression
 569 differences, explaining ~59% of the overall variance in gene expression ($R^2 = 0.59$, F
 570 $= 41.22$, $p = 0.001$), reflecting our strong stage-specific transcriptional patterns. In
 571 contrast, neither leachate level ($R^2 = 0.02$, $F = 1.09$, $p = 0.338$) nor the interaction
 572 between leachate and stage ($R^2 = 0.04$, $F = 0.81$, $p = 0.679$) significantly influenced
 573 the multivariate expression structure. Residual variation accounted for 35% of the

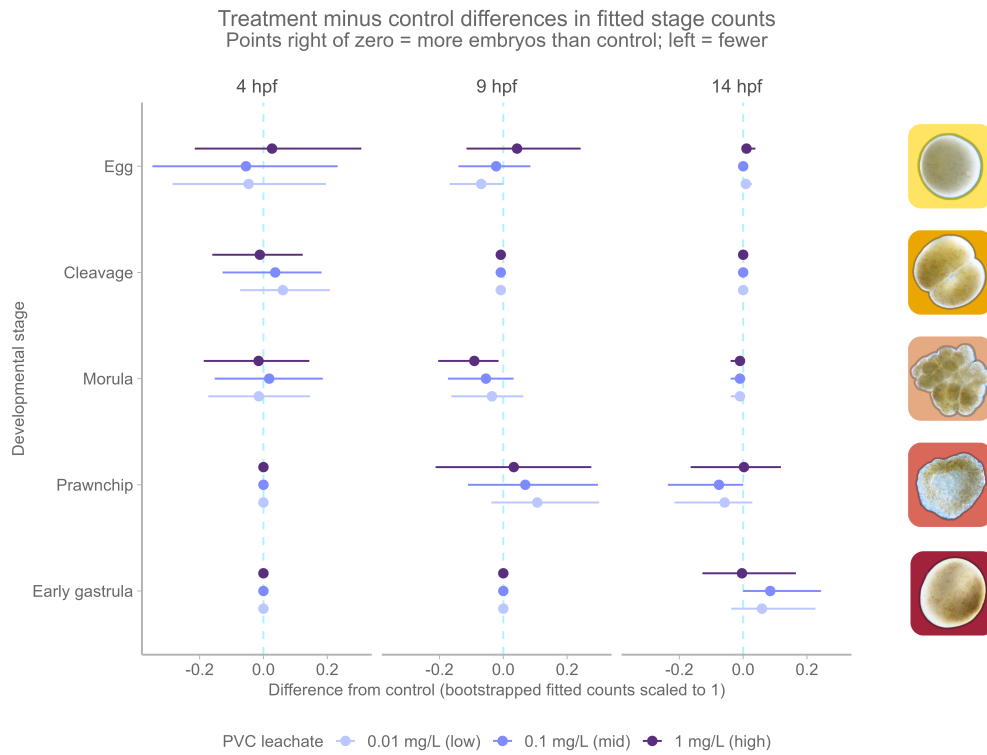


Figure 5: Bootstrap predicted effects of PVC leachate on embryo developmental stage composition over time. Points show multivariate GLM-predicted differences in embryo counts for each developmental stage (egg, cleavage, morula, prawnchip, early gastrula) between leachate treatments (0.01, 0.1, 1 mg/L) and the control at 4, 9, and 14 hpf. Error bars indicate 95% confidence intervals over 500 bootstrap iterations. The vertical dashed line at zero denotes no difference from control; values to the right indicate increased counts relative to control, and values to the left indicate decreases.

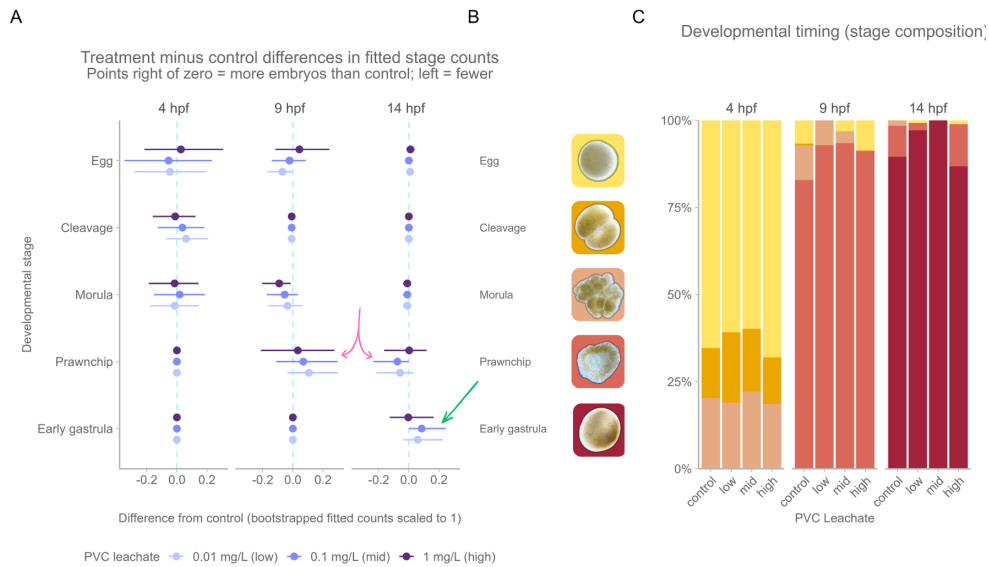


Figure 6: A. Bootstrap-predicted effects of PVC leachate on embryo developmental stages over time. The pink arrow points to more prawnchip embryos found in the low and middle leachate levels relative to control at 9 hours post-fertilization (hpf), and less at 14 hpf. Green arrow points to more early gastrula stage embryos found in the low and middle leachate levels relative to the control at 14 hpf. Points show model-estimated differences in embryo counts (leachate vs. control) for each stage (egg, cleavage, morula, prawnchip, early gastrula) at 4, 9, and 14 hpf across three levels (0.01, 0.1, 1 mg/L). Error bars show 95% confidence intervals from 500 bootstrap iterations. The dashed line indicates no difference from control; values above zero indicate increases and values below zero indicate decreases. B. Legend of embryo stages. C. Proportion stacked barplot showing the percent makeup of surviving embryo stages at each developmental endpoint sampled (4, 9, 14 hpf). Notice how there are relatively more cleavage in low and mid levels at 4 hpf, relatively more prawnchip in low and mid levels at 9 hpf, and relatively more early gastrula in low and mid levels at 14 hpf.

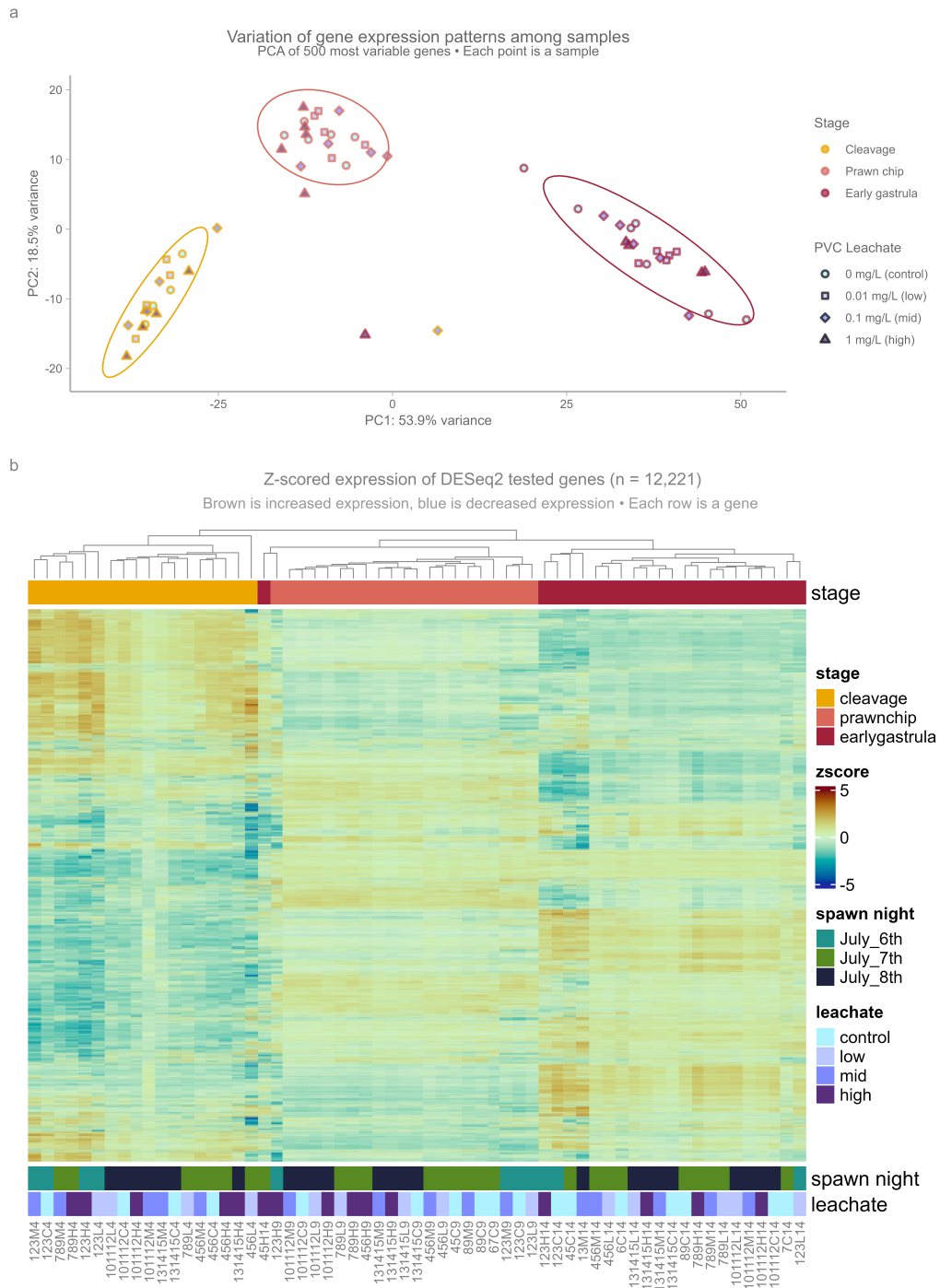


Figure 7: Principal Component Analysis (PCA) of VST-normalized gene expression across all samples.

574 total variance. Tests for homogeneity of multivariate dispersion revealed significant
 575 within-stage differences ($F = 15.03$, $p = 0.001$, 999 permutations), suggesting that
 576 the observed PERMANOVA stage effect reflects a combination of strong centroid
 577 separation *and* variable spread. Despite differences in dispersion, the magnitude of
 578 the stage effect and the clear separation observed in PCA indicate that developmental
 579 stage represents robust, biologically meaningful early developmental gene expression
 580 programs.

581 3.2.2 *DEG clusters*

582 There are ~56K genes in the *M. capitata* genome (Stephens et al., 2022), of which we
 583 filtered to a test group of 12,221 genes. Of the 12,221 genes tested with DESeq2, we
 584 found 130 were differentially expressed due to the interaction between leachate and
 585 stage. We will refer to these as the leachate-responsive DEGs.

586 Among the 130 leachate-responsive DEGs, trajectory-based clustering using the
 587 DEGreport v 1.44.0 R package and the degPatterns function found 128 genes that
 588 fit into one of three gene expression patterns (Figure 8). These expression patterns
 589 are structured by developmental timing, with groups exhibiting highest relative
 590 transcript abundance at cleavage (31 genes), prawn-chip (25 genes), or early gastrula
 591 (75 genes) stages, respectively (Figure 8 A-C). Two leachate-responsive DEGs did not
 592 fit into any of these patterns, and were excluded from downstream analysis. Leachate
 593 effects within these clusters were modest, with leachate treatments exhibiting subtle
 594 deviations compared to the control samples most evident at stages where baseline
 595 expression was lowest.

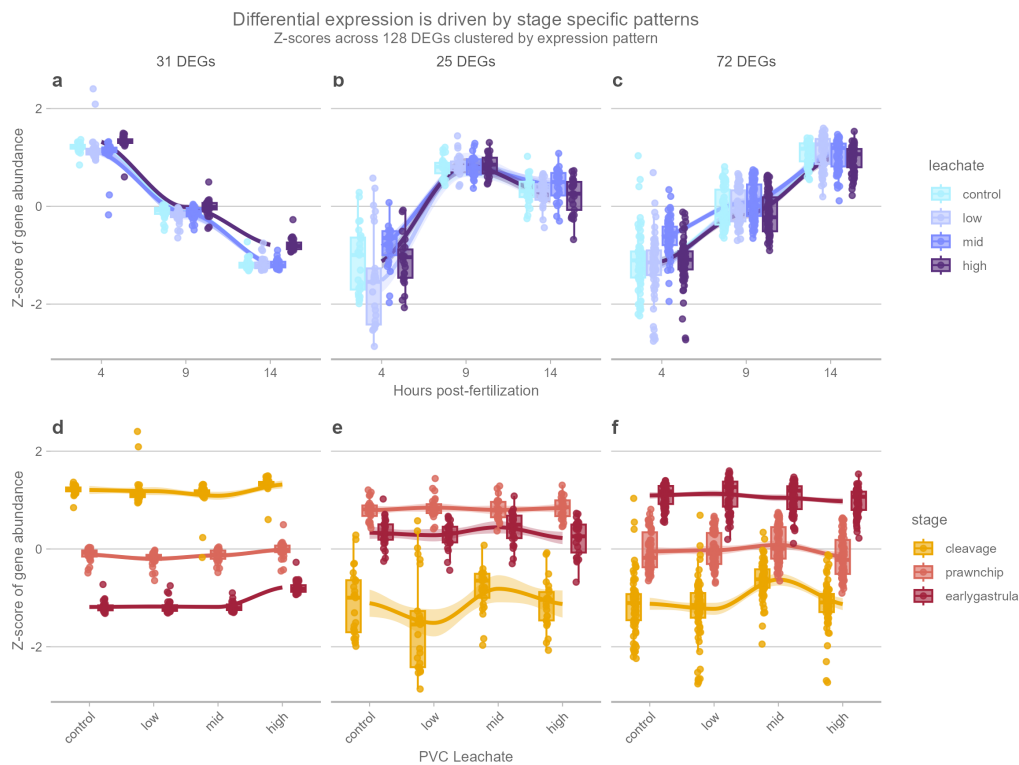


Figure 8

596 In contrast, the DEGs associated with development (10,793 genes) were analyzed
 597 using weighted gene co-expression network analysis (WGCNA) with the WGCNA v
 598 1.73 R package (Langfelder & Horvath, 2008), which identified six modules ranging
 599 in size from 326 to 2,805 genes. Module eigengene profiles revealed four dominant
 600 developmental programs (expression patterns): a cleavage-high program characterized
 601 by decreases in expression over developmental time, two prawn-chip-associated
 602 programs showing either up-regulation (hump or inverted-U-shaped expression
 603 profile) or mid-stage suppression (valley or U-shaped expression profile), and late
 604 developmental programs with increasing expression toward early gastrulation. These
 605 modules represent coordinated transcriptional programs associated with embryonic
 606 progression and were retained for downstream GO functional enrichment analyses.
 607 149 developmental DEGs were not assigned to a cluster in the WGCNA, and were
 608 excluded from downstream analysis.

609 All 130 leachate-responsive DEGs are also listed in the genes that change across
 610 developmental stage; indicating that the shifts in gene expression detected across
 611 leachate treatments are nested within the larger shifts in gene expression occurring
 612 over developmental time.

613 **3.2.3 Summary of GOslim terms**

614 Of the 12,221 genes included in the DESeq2 testing universe, 6,846 (56%) had at
 615 least one Gene Ontology (GO) annotation. GO annotation coverage among leachate-
 616 responsive differentially expressed genes (DEGs) was high across all stage-associated
 617 expression patterns, including 27/31 (87%) genes in the cleavage-associated (4 hpf)
 618 pattern, 19/25 (76%) genes in the prawnchip-associated (9 hpf) pattern, and 62/72
 619 (86%) genes in the early gastrula-associated (14 hpf) pattern. Goseq enrichment
 620 analysis did not identify any significantly enriched biological processes after correction
 621 for gene-length bias ($q > 0.05$ for all comparisons). Therefore, GO Slim categories
 622 were used descriptively to summarize the functional identities of leachate-responsive
 623 genes within each developmental expression pattern (Figure 9).

624 The 31 leachate-responsive DEGs exhibiting the cleavage (4 hpf) expression pattern,
 625 in which transcript abundance decreased across development (4>9>14 hpf), were
 626 dominated by GO Slim terms related to early developmental regulation and nuclear
 627 organization, including anatomical structure development, cell differentiation, meiotic
 628 nuclear division, chromosome segregation, and chromatin organization. Additional
 629 cleavage-associated terms included intracellular protein transport and nervous system
 630 process. Together, these functions suggest that leachate-responsive genes expressed
 631 most strongly during cleavage were associated with maternally provisioned develop-
 632 mental programs, chromosomal organization, and cell division fidelity during early
 633 embryogenesis.

634 In contrast, the prawnchip expression pattern, characterized by genes peaking tran-
 635 siently at 9 hpf (4<9<14 hpf), contained fewer total leachate-responsive DEGs (25)
 636 and was characterized by genes involved in lipid metabolic process, signaling, and
 637 programmed cell death. These functions suggest a transient shift toward metabolic
 638 and stress-associated responses during the prawnchip stage.

639 The early gastrula (14 hpf) expression pattern, in which transcript abundance
 640 increased across development (4<9<14 hpf), contained the largest number of leachate-
 641 responsive DEGs (72 genes). Dominant GO Slim categories included anatomical
 642 structure development, cell differentiation, signaling, vesicle-mediated transport,
 643 mitotic cell cycle, cytoskeleton organization, and protein-containing complex assembly
 644 (). These functions are consistent with increased cellular remodeling, intracellular
 645 trafficking, and structural reorganization during gastrulation.

646 Several GO Slim categories, including anatomical structure development, cell differ-
 647 entiation, DNA-templated transcription, regulation of DNA-templated transcription,

648 reproductive process, immune system process, and signaling, were consistently
 649 observed across all three developmental expression patterns, suggesting that core
 650 developmental and regulatory processes were responsive to PVC leachate exposure
 651 throughout embryogenesis. However, stage-specific differences in the dominant func-
 652 tional categories indicate that the biological consequences of leachate exposure varied
 653 across developmental time, with cleavage-stage responses emphasizing chromosomal
 654 and nuclear regulation, prawnchp responses reflecting transient metabolic and stress-
 655 associated processes, and early gastrula responses dominated by cellular activation
 656 and structural reorganization.

Counts of Leachate-Responsive Differentially Expressed Genes described by Gene Ontology (GO) Slim Terms

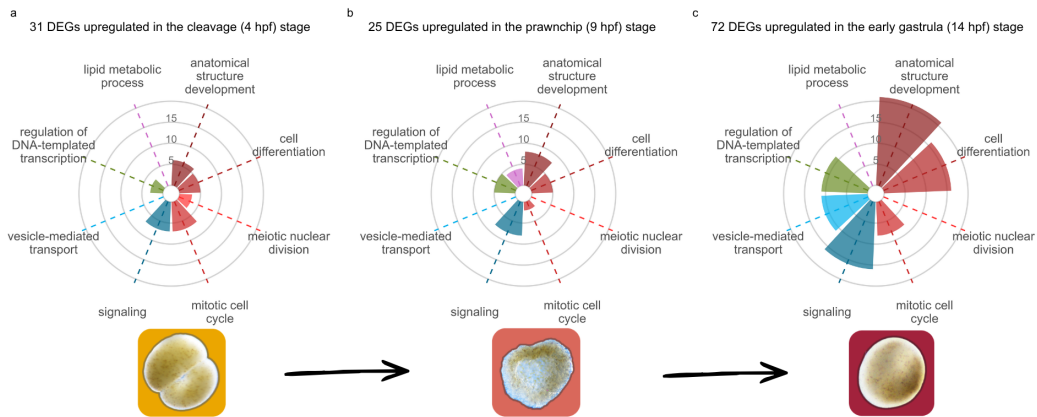


Figure 9: Functional annotation of PVC leachate-responsive genes across developmental stage-specific expression clusters. Gene counts were grouped into GOSlim categories for genes with peak expression during a) cleavage (31 DEGs) annotated to mitotic cell cycle, signaling, anatomical structure development, and cell differentiation. b) prawnchp (25 DEGs) annotated in anatomical structure development and signaling. c) early gastrula (72 DEGs) annotated in anatomical structure development, cell differentiation, signaling and vesicle-mediated transport, and transcriptional regulation.

657 3.3 H_3 : Microbiome

658 3.3.1 *Alpha diversity*

659 A two-way analysis of variance (ANOVA) revealed no significant effects of PVC
 660 leachate level, developmental stage, or their interaction on Shannon diversity. Differ-
 661 ences in Shannon diversity among leachate treatments were not statistically significant
 662 (F , = 1.25, p = 0.302), nor were differences among developmental stages (F , =
 663 1.11, p = 0.339). Similarly, the leachate \times stage interaction was not significant (F ,
 664 = 0.33, p = 0.919), indicating that leachate did not affect microbial alpha diversity
 665 across stages. A two-way ANOVA revealed a significant effect of developmental stage
 666 on Faith's phylogenetic diversity, with post hoc Tukey HSD tests showing reduced
 667 phylogenetic diversity at 14 hpf compared to 4 hpf (p_{adj} = 0.04).

668 Alpha diversity remained stable across treatments, indicating limited sensitivity of
 669 within- sample microbial diversity to leachate exposure or developmental progression.

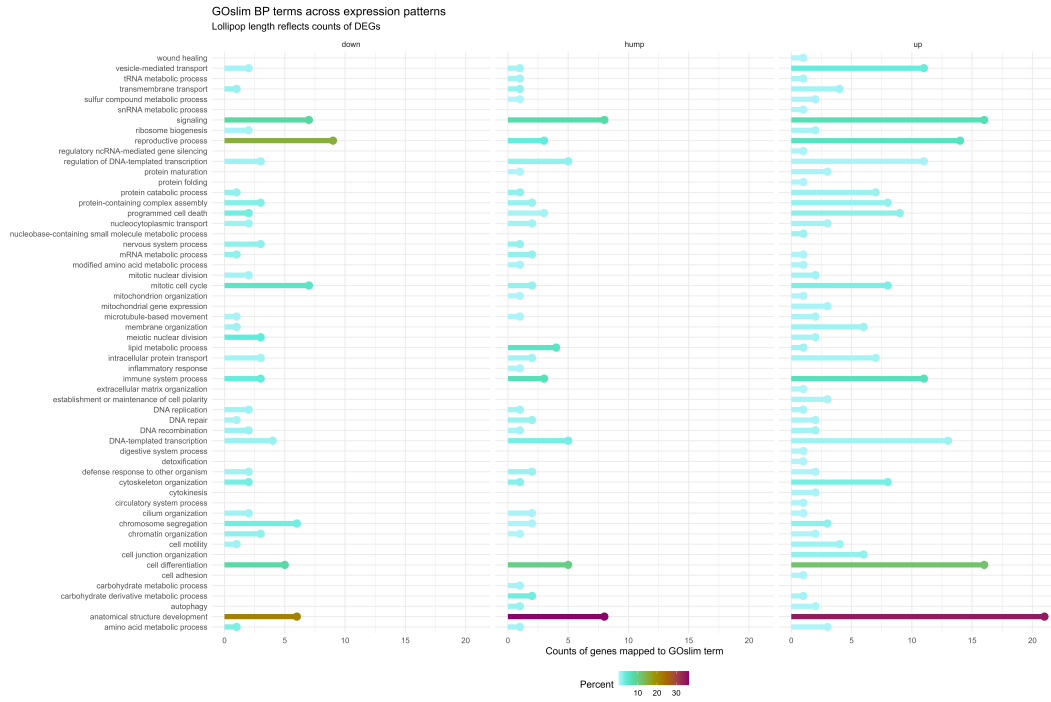


Figure 10: Counts of DEGs binned into GOSlim Biological Process (BP) terms and colored by percent enrichment

670 Following recommendations from Gloor et al. (2017), we used the centered log-ratio
 671 (CLR) transformation to convert our data to Euclidean space to an Aitchison distance
 672 (Euclidean distance on CLR-transformed data) matrix. We then performed a PCA
 673 on the Aitchison distance matrix to visually assess multivariate differences between
 674 samples (Figure 13 A-C).

675 **3.3.2 Betadispersion, PERMANOVA & Beta Diversity**

676 Homogeneity of multivariate dispersion was assessed using the Aitchison distance
 677 matrix with the betadisper() function from the vegan package prior to conducting
 678 a PERMANOVA to determine if microbiome sample ASV composition differed
 679 significantly across developmental stage and leachate level.

680 PERMANOVA tests for differences in group centroids in multivariate space but
 681 assumes that within-group dispersion is comparable across groups. If dispersions differ
 682 significantly, PERMANOVA may detect differences driven by unequal variability
 683 rather than true shifts in community composition. By first evaluating whether average
 684 distances to group centroids differed across groups, we determined whether the
 685 assumption of homogeneous dispersion was met.

686 The permutation test for homogeneity of multivariate dispersions revealed no
 687 significant difference in dispersion across leachate ($F_{3,59} = 0.14$, $p = 0.939$, 999
 688 permutations), stage ($F_{2,60} = 1.0498$, $p = 0.36$, 999 permutations), or the interaction
 689 between leachate and stage ($F_{11,51} = 0.35$, $p = 0.971$, 999 permutations), indicating
 690 groups have equal variance and meet the assumptions of PERMANOVA. However, we
 691 found that multivariate dispersion differed significantly across spawn nights ($F_{2,60} =$
 692 6.29 , $p = 0.003$, 999 permutations). Microbiome composition was clearly more varied
 693 on July 7th compared to July 6th and 8th, evident by the larger spread around the
 694 group centroid (Figure 12 A).

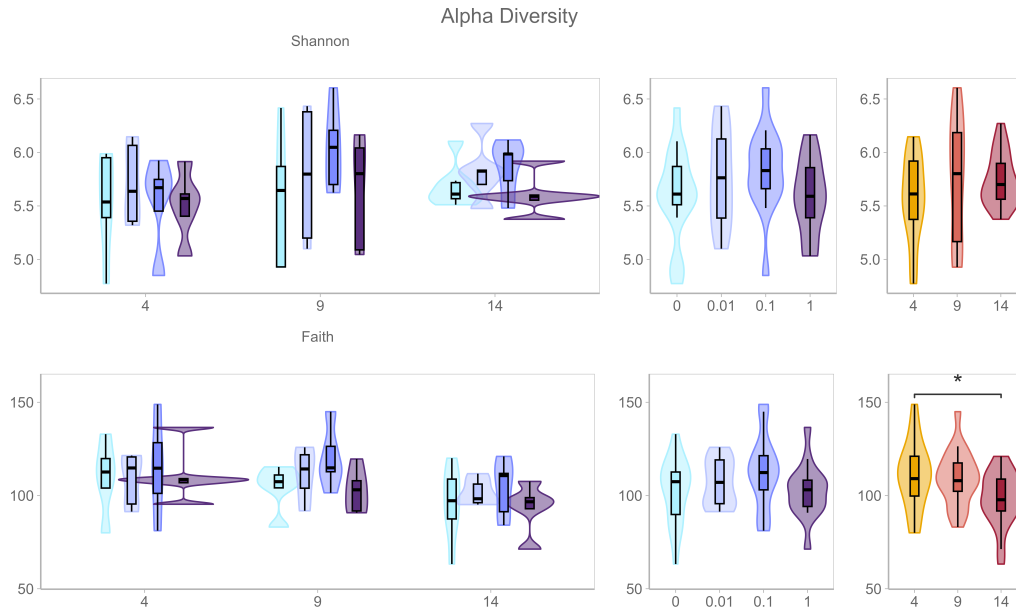


Figure 11: Alpha diversity metrics across PVC leachate treatments and developmental stages in coral embryo-associated microbial communities. Shannon diversity (top row) and Faith's phylogenetic diversity (bottom row) are shown across the interaction between PVC leachate treatment and developmental stage (left panels), PVC leachate treatment (center panels), and stage-specific distributions (right panels). Violin plots represent the distribution of samples within each group, with embedded boxplots indicating medians and interquartile ranges. Developmental stage had a stronger influence on alpha diversity patterns than PVC leachate treatment. Shannon diversity remained relatively stable across stages and treatments, whereas Faith's phylogenetic diversity differed significantly among developmental stages, with reduced phylogenetic diversity observed at 14 hpf relative to 4 hpf ($p_{adj} = 0.04$). No strong treatment-associated shifts in alpha diversity were observed across PVC leachate levels.

Principle Coordinates Analysis (PCoA)
of Within-Group Beta Diversity Dispersion

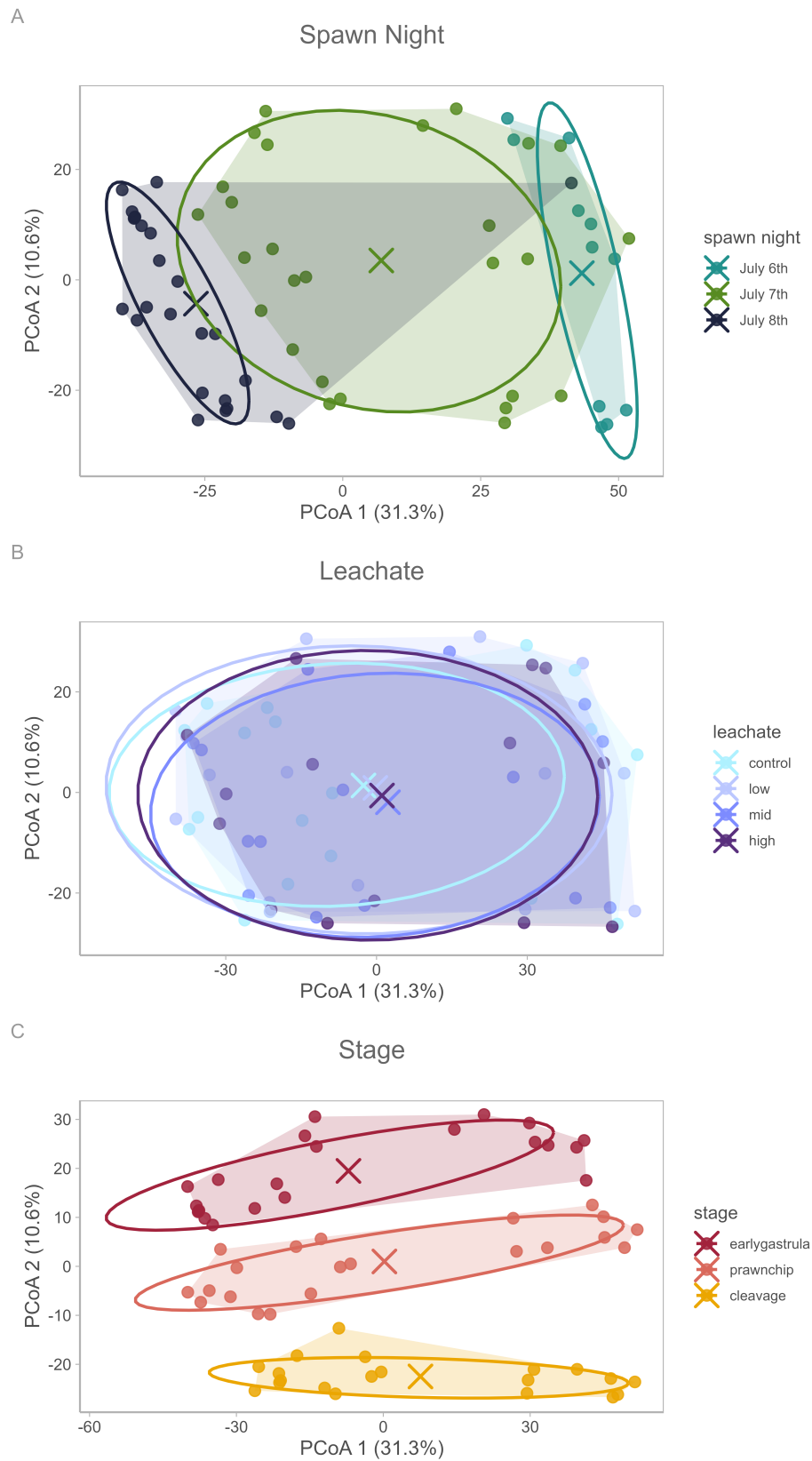


Figure 12: A. betadispersion at spawn night B. betadispersion by leachate C. betadispersion by stage

695 This finding prompted us to control for spawn night as a nuisance factor in our exper-
 696 iment by restricting permutations of samples among others within the same spawn
 697 night via strata, which accounts for the non-independence of samples collected on the
 698 same night when calculating the significance of our factors of interest (developmental
 699 stage and leachate level).

700 We conducted a community composition analysis using a PERMANOVA conducted
 701 on Aitchison distances with 999 permutations, stratified by spawn night (Figure 13
 702 A). It revealed a significant effect of developmental stage on community composition
 703 ($F_{2,51} = 3.84$, $R^2 = 0.119$, $p = 0.001$, 999 permutations), indicating that stage ex-
 704 plained approximately 11.9% of the variation in multivariate structure (Figure 13 C).
 705 In contrast, leachate treatment had no significant effect ($F_{3,51} = 0.84$, $R^2 = 0.039$,
 706 $p = 0.297$, Figure 13 B), and there was no significant leachate \times stage interaction ($F_{6,51} = 0.51$, $R^2 = 0.048$, $p = 1.000$).

708 **3.3.3 Differentially abundant and prevalent bacterial taxa**

709 To identify individual taxa associated with leachate exposure over developmental time,
 710 MaAsLin3 generalized linear mixed models were applied at the genus (L6) taxonomic
 711 level using the model formula “abundance|prevalence ~ leachate * hpf + reads +
 712 (1|spawn_night)”. This framework tested both abundance and prevalence responses
 713 while accounting for sequencing depth and variation among spawn nights.

714 Across 885 bacterial genera tested, eight genera showed significant associations with
 715 leachate exposure in the abundance model and eight genera showed significant asso-
 716 ciations in the prevalence model after filtering for models without fitting errors and
 717 joint false discovery rates of $q < 0.1$. Seven of these genera overlapped between the
 718 abundance and prevalence analyses, indicating that most responsive taxa exhibited
 719 coordinated shifts in both relative abundance and detection probability across treat-
 720 ments. Responsive taxa included members of the genera *Tropicibacter*, *Sulfitobacter*,
 721 *Peredibacter*, *Pontibacterium*, PS1 clade taxa, uncultured *Neisseriaceae*, and Marine
 722 Methylophilic Group 3 (Figure 14). One genus within the *Longimicrobiaceae* was
 723 uniquely significant in prevalence models (Figure 15), while *Leeuwenhoekiella* was
 724 uniquely significant in abundance models (Figure 14).

725 In contrast, an alternative model treating leachate level as a continuous linear pre-
 726 dictor detected no significant leachate-associated taxa. The absence of significant
 727 linear responses, combined with significant associations in the categorical model,
 728 suggests that bacterial responses to PVC leachate were non-linear across exposure
 729 levels. Several taxa displayed the strongest shifts at low or intermediate leachate
 730 levels compared to the high leachate level, rather than a monotonic relationship across
 731 the level gradient, consistent with our hypothesis that we would observe low-dose
 732 responses.

733 Although only a small proportion of taxa responded significantly to leachate exposure
 734 (0.9% of genera tested), these results exceeded expectations under random chance
 735 given the applied false discovery threshold and stringent filtering criteria. Relative
 736 abundance and prevalence visualizations further indicated that responsive taxa varied
 737 across developmental stages, with some genera exhibiting stage-specific increases or
 738 decreases in abundance and detection probability under leachate exposure. Overall,
 739 these findings suggest that PVC leachate did not broadly restructure the embryonic
 740 microbiome, but instead produced targeted and non-linear shifts in a limited subset of
 741 bacterial taxa.

742 **3.3.4 Predicted functional enrichment**

743 Differential abundance and prevalence testing of PICRUSt2-predicted MetaCyc
 744 pathways identified multiple microbial functional pathways associated with PVC
 745 leachate exposure and stage-dependent responses. Functional shifts were distributed
 746 across pathways involved in methanogenesis, carbon fixation, aromatic compound

Principal Coordinates Analysis (PCoA) of Aitchison Beta Diversity

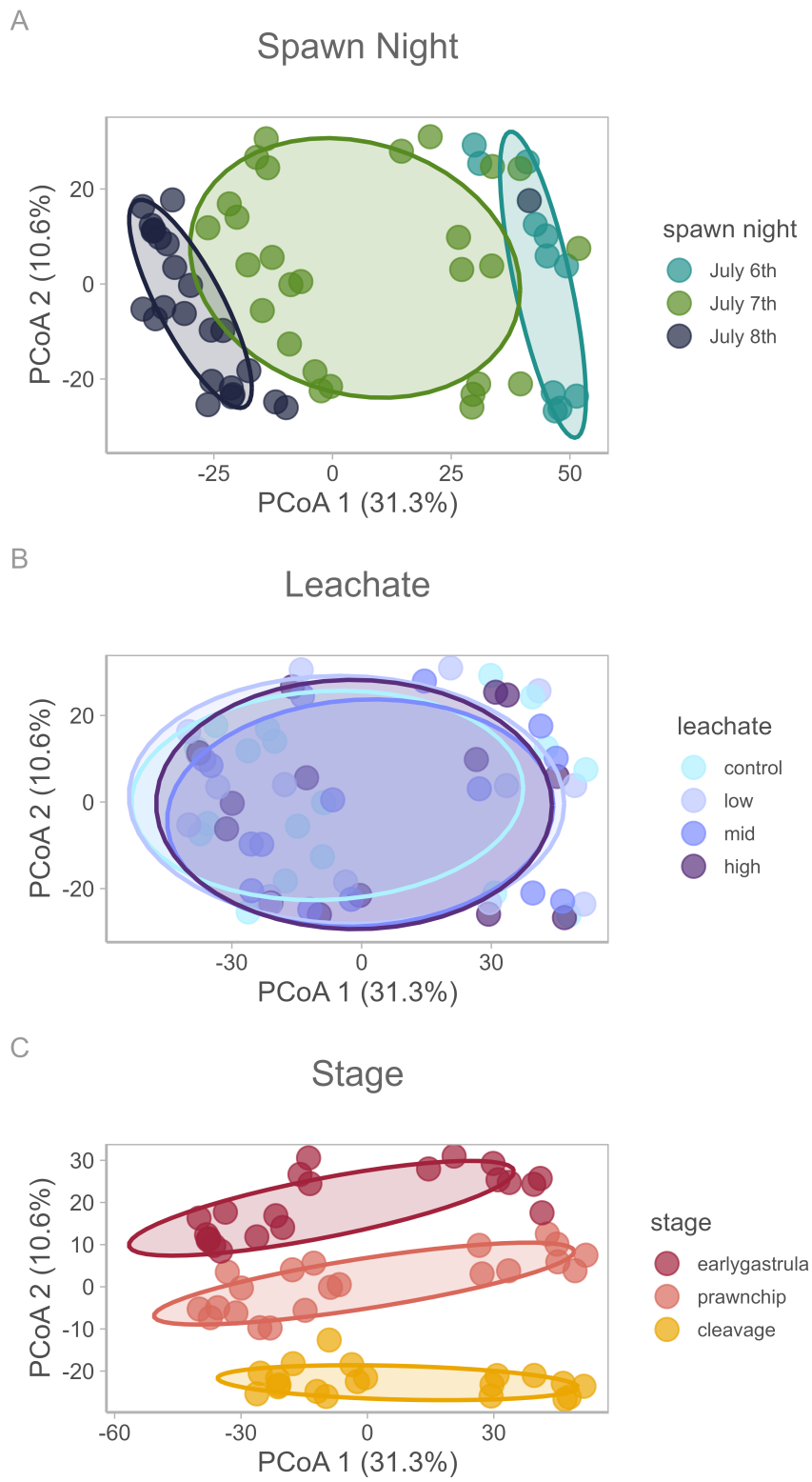


Figure 13: A. B. C.

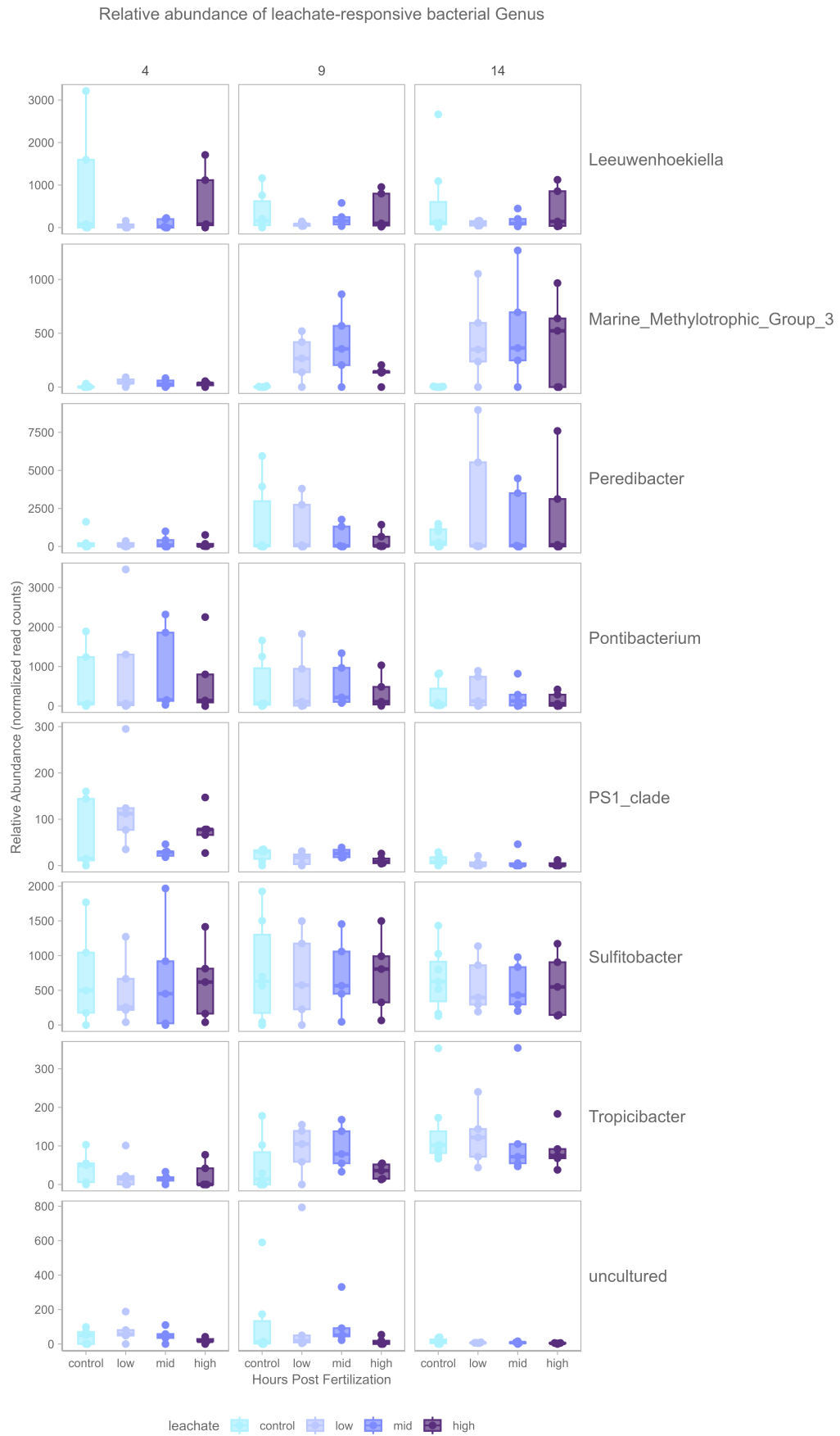


Figure 14

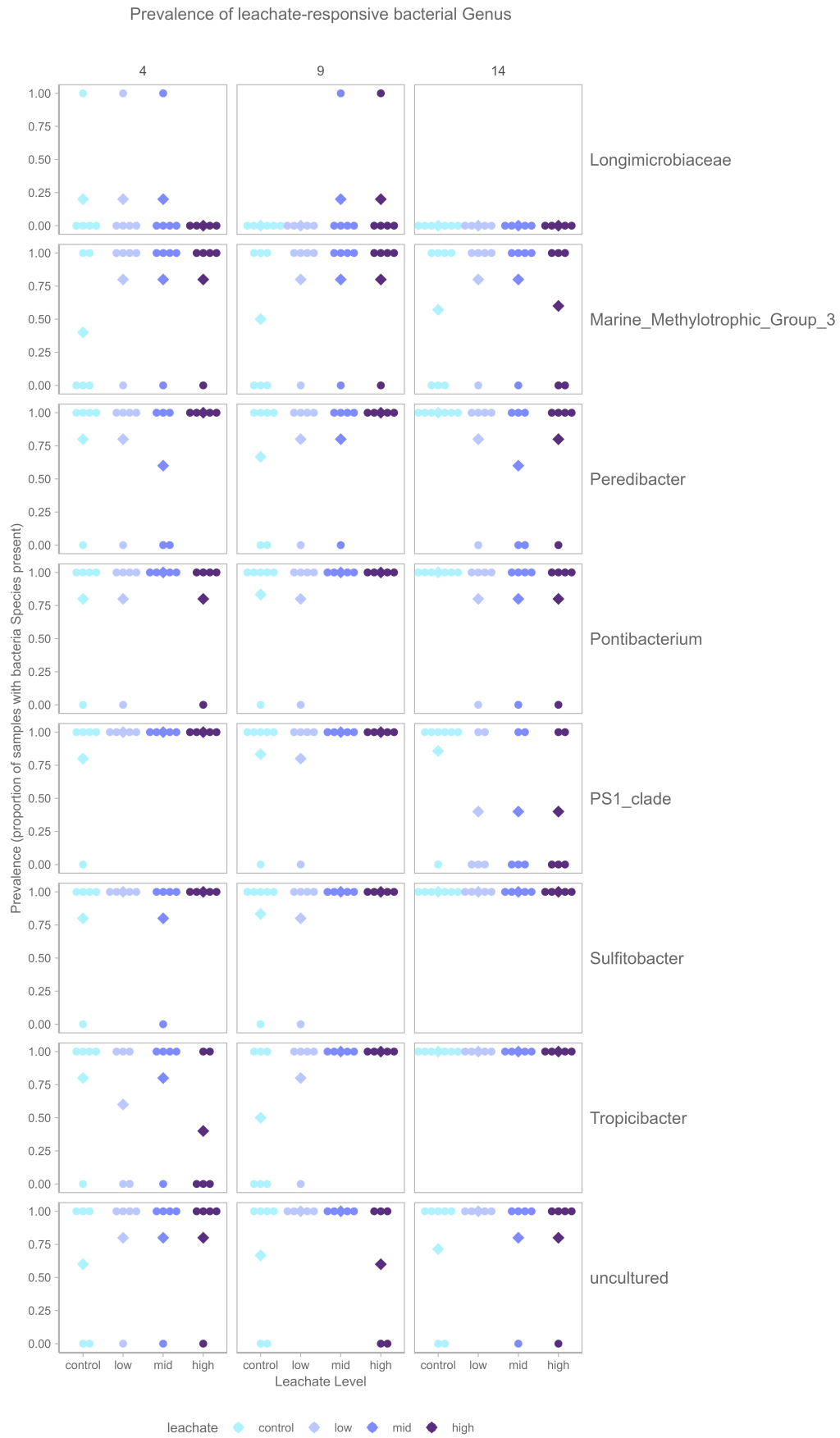


Figure 15

747 degradation, chlorinated compound degradation, and precursor metabolite biosynthe-
748 sis.

749 Several significant pathways were associated with methane metabolism and anaerobic
750 carbon cycling, including the superpathway of C1 compound oxidation to CO₂
751 (PWY-1882), methyl-coenzyme M oxidation to CO₂ I (PWY-5209), and the reductive
752 acetyl-CoA pathway in autotrophic methanogens (PWY-7784). These pathways are
753 primarily associated with archaeal methanogenic and methylotrophic metabolism and
754 suggest shifts in microbial functional potential related to anaerobic respiration and
755 carbon processing in the *Marine Methylotrophic Group 3* differentially abundant taxa.

756 Additional predicted pathways involved aromatic and chlorinated compound degra-
757 dation, including cinnamate and hydroxycinnamate degradation (PWY-6690),
758 3-phenylpropanoate degradation (HCAMHPDEG-PWY; PWY0-1277), toluene degra-
759 dation (TOLUENE-DEG-3-OH-PWY), pentachlorophenol degradation (PCPDEG-
760 PWY), and dichlorobenzene degradation (14DICHLORBENZDEG-PWY; PWY-6084).
761 Many of these pathways are associated with bacterial degradation of aromatic
762 hydrocarbons and chlorinated compounds, which are commonly linked to anthro-
763 pogenic pollution and industrial contaminants. The enrichment of pathways related
764 to aromatic and chlorinated compound metabolism suggests that PVC leachate
765 exposure may favor microbial taxa capable of metabolizing plastic-associated organic
766 compounds or responding to chemically stressful environments.

767 Predicted pathways associated with lipid metabolism and signaling were also detected,
768 including phosphatidate metabolism as a signaling molecule (PWY-7039). Because
769 PICRUST2 predicts functional *potential* from taxonomic composition rather than
770 directly measuring gene expression or metabolism, these results represent *inferred*
771 functional capacity rather than confirmed metabolic activity.

772 4 Discussion

773 Plastic pollution is an emerging threat to coral reefs, not only as a physical stressor
774 but also as a source of chemical contaminants that may disrupt sensitive developmen-
775 tal processes. Here, we show that environmentally relevant levels of PVC leachate can
776 trigger subtle shifts in developmental timing, gene expression, and specific microbial
777 taxa in *Montipora capitata* within the first 14 hours of development, despite no
778 detectable effects on survival or visible abnormalities. These findings reveal that
779 plastic-derived chemicals can induce early, sublethal biological responses that are
780 missed by traditional toxicity endpoints, highlighting previously under-explored
781 mechanisms by which plastic pollution may already be impacting coral resilience.

782 4.1 *H*₁: Coral development slightly accelerated at low and moderate PVC 783 leachate exposures

784 The effects of leachate varied across both level and developmental time. The strongest
785 treatment-dependent response was observed during the prawnchip stage, particularly
786 under low and moderate PVC leachate exposure. These results indicate that PVC
787 leachate did not broadly disrupt embryogenesis or induce developmental arrest, but
788 instead caused subtle, stage-specific shifts in developmental pace. Developmental tim-
789 ing in marine larvae is highly plastic and responds to environmental conditions, such
790 as temperature, with warmer conditions often accelerating embryonic development
791 and influencing dispersal and recruitment success (O'Connor et al., 2007; Woolsey et
792 al., 2013). Our findings suggest that plastic-derived chemicals may similarly influence
793 developmental timing by interacting with endocrine-like signaling pathways involved
794 in growth and differentiation (Ann M. Tarrant (2007), Figure 9). The fact that
795 responses were strongest at low and intermediate levels, rather than at the highest
796 exposure level, is consistent with non-monotonic response patterns commonly reported
797 for endocrine-disrupting compounds such as plasticizers and other PVC additives
798 (Vandenberg et al., 2012).

799 One prior study found that weathered polypropylene microplastics minimally reduced
 800 fertilization success and increased embryo abnormalities in a non-dose dependent
 801 manner in the reef-building coral *Acropora tenuis* (Berry et al., 2019). Furthermore,
 802 exposure to high-density polyethylene (HDPE) leachate reduced larval survival and
 803 settlement in both *M. capitata* and *Porites* species, with higher levels (200mg/L)
 804 of high-density polyethylene (HDPE) leachate treatments paradoxically promoting
 805 settlement, potentially through attraction to chemical cues associated with degrading
 806 plastics (Wilkins & Richmond (2025)).

807 Our findings suggest that the prawnchips stage represents a critical developmen-
 808 tal bottleneck in *Montipora capitata*, as embryos at this stage are more prone to
 809 fragmentation, likely due to the thin single-cell epithelial layer that characterizes
 810 this bizarre stage. We observed more torn embryos at 9 hpf relative to 4 or 14 hpf
 811 regardless of treatment (Figure 4 C), indicating that this stage may be particularly
 812 vulnerable to mechanical damage or developmental abnormalities. In some corals,
 813 embryo fragmentation has been proposed as a mechanism for increased reproductive
 814 output, provided that fragmented embryos remain viable and continue to develop as
 815 twins (Heyward & Negri, 2012).

816 Our morphological findings are supported by our transcriptomic data, which showed
 817 that leachate-responsive genes during early development were associated with cellular
 818 signaling and mitotic cell cycle processes (Figure 9, Figure 10), pathways that are
 819 central to regulating developmental progression.

820 Ramakrishnan & Wayne (2008) demonstrated that low-dose bisphenol A (BPA)
 821 exposure accelerated embryonic development, advanced hatching, and accelerated
 822 reproductive maturation in medaka (*Oryzias latipes*), with these effects mediated
 823 through thyroid hormone signaling pathways rather than classical estrogenic signaling.
 824 Similarly, Anselmo et al. (2011) reported that triphenyltin (TPT) and dibutyltin
 825 (DBT), two endocrine-disrupting chemicals commonly added to PVC products,
 826 accelerated metamorphosis in the sea urchin *Psammechinus miliaris*. Together, these
 827 studies suggest that plastic-associated endocrine-disrupting compounds can accelerate
 828 or influence developmental timing by interfering with signaling pathways that regulate
 829 growth and differentiation.

830 An alternative explanation is that low and moderate levels of PVC leachate exposure
 831 selectively favored embryos that were already developing more rapidly, resulting
 832 in an apparent shift in developmental progression rather than a true acceleration
 833 of development at the individual level. Distinguishing between true developmental
 834 acceleration and selective survival would require longitudinal tracking of individual
 835 embryos and larvae.

836 Notably, most previous studies examining plastic leachate effects on marine inverte-
 837 brates have reported developmental disruption, arrest, or delay rather than *accelerated*
 838 development. For example, Paganos et al. (2023) documented severe embryotoxicity
 839 and morphological abnormalities in *Strongylocentrotus purpuratus* embryos exposed
 840 to PVC pellet leachate, with zinc identified as a primary driver of toxicity. Similarly,
 841 Jimenez-Guri et al. (2023) reported concentration-dependent disruption of axial
 842 formation, cell specification, and morphogenesis across multiple animal phyla, includ-
 843 ing cnidarians. However, the concentrations used in these studies were substantially
 844 higher than those tested in our study. It is possible that high levels of PVC leachate
 845 overwhelm subtle signaling-mediated effects on developmental timing responses and
 846 instead produce more pronounced toxic responses.

847 **4.2 H₂: PVC leachate impacted genes responsible for development, gene** 848 **regulation, and cellular communication**

849 Early coral embryogenesis is characterized by rapid cell division, gastrulation, and
 850 extensive use of maternally provisioned resources (E. Chille et al., 2021; Huffmyer

851 et al., 2023). Our results showed that developmental stage explained substantially
852 more transcriptomic variation than PVC leachate exposure. Rather than causing
853 broad disruption of gene expression, PVC leachate induced comparatively subtle
854 molecular responses embedded within the larger signal of gene expression across
855 development. This pattern is consistent with developmental canalization, or the idea
856 that early embryos may be partially buffered against environmental perturbations
857 through maternal mRNA provisioning (E. Chille et al., 2021; E. E. Chille et al., 2022),
858 allowing core developmental processes to remain stable despite exposure to complex
859 contaminants.

860 Although overall gene expression remained largely unchanged, we identified 130
861 leachate-responsive genes associated with cellular signaling, transcriptional regulation,
862 vesicle-mediated transport, lipid metabolism, and mitotic cell cycle activity (Figure 9),
863 suggesting that PVC leachate primarily affected regulatory and cellular maintenance
864 pathways rather than causing widespread developmental disruption. The stage-specific
865 nature of these responses further indicates that sensitivity to leachate exposure
866 changes across embryogenesis, likely reflecting differences in developmental state, ener-
867 getic demand, or the timing of key cellular transitions. For example, cleavage-stage
868 responses were associated with chromosomal and nuclear organization (Figure 10
869 A), whereas later gastrulation-stage responses were more strongly linked to cellular
870 remodeling, signaling, and intracellular transport (Figure 10 C).

871 Among the leachate-responsive genes were several associated with G protein-coupled
872 receptor (GPCR) signaling and related developmental signaling pathways. (Mor-
873 gan et al., 2022) exposed the sea anemone *Exaiptasia diaphana* to oxybenzone, a
874 common sunscreen additive, and benzyl butyl phthalate, a plasticizer, and found
875 altered expression of candidate endocrine-disruption biomarker genes associated with
876 pathways involving GPCRs. Their study focused on genes involved in steroid hormone
877 biosynthesis, cholesterol transport, immunity, phagocytosis, and Hedgehog signaling,
878 including Niemann-Pick C type 2 (NPC2), Cathepsin L (CTSL), Smoothed (SMO),
879 Desert Hedgehog (DHH), Zinc finger protein GLI2 (GLI2), and Vitellogenin (VTG).
880 Although none of the leachate-responsive *Montipora capitata* transcripts mapped di-
881 rectly to the candidate genes identified by (Morgan et al., 2022), several DEGs carried
882 functional annotations associated with similar signaling and regulatory pathways,
883 including GPCR-mediated signaling, steroid hormone-associated signaling, and Wnt
884 pathway regulation.

885 To find these in our system, we filtered leachate-responsive DEGs for gene ontology
886 (GO) terms associated with GPCR and related signaling processes, including “G
887 protein”, “GPCR”, “signal transduction”, “receptor”, “transmembrane signaling”,
888 “second messenger”, “hedgehog”, “adenylate cyclase”, “Wnt”, and “cell signaling”.
889 This search identified 74 GO terms related to GPCR-associated signaling, including
890 regulation of G protein-coupled receptor signaling pathways, steroid hormone receptor
891 signaling pathways, nuclear receptor-mediated steroid hormone signaling, and canon-
892 ical Wnt signaling. These GO terms mapped to 32 of the 130 leachate-responsive
893 DEGs, including 6 genes associated with cleavage-stage expression patterns, 8 asso-
894 ciated with prawnchips-stage patterns, and 16 associated with early gastrula-stage
895 patterns.

896 GPCR signaling pathways act like switches that pass signals inside the cell. They
897 function through membrane-bound receptors that detect extracellular signals such
898 as peptides, hormones, or environmental cues and activate intracellular signaling
899 cascades through G proteins and second messengers such as cyclic AMP and calcium
900 signaling. These signaling pathways regulate downstream transcriptional programs
901 involved in cell differentiation, morphogenesis, developmental timing, and stress
902 responses (Lauretta C. Grasso et al., 2008). The presence of GO terms associated
903 with Wnt and Hedgehog signaling is particularly notable because these pathways are

904 highly conserved regulators of embryonic axis formation, tissue patterning, and cell
905 fate determination across metazoans.

906 Corals and other cnidarians lack centralized endocrine organs found in vertebrates, yet
907 possess diverse peptide-mediated signaling systems that may function in endocrine-like
908 regulation (Thiel et al., 2023; Twan et al., 2006). In cnidarians, neuropeptides and
909 other extracellular signaling molecules are thought to interact heavily with GPCR
910 pathways to coordinate developmental regulation, environmental sensing, metabolism,
911 and larval settlement (L. C. Grasso et al., 2001; Hambleton et al., 2018). Because
912 GPCR pathways can amplify subtle extracellular signals into large downstream
913 transcriptional responses through second messenger cascades (Civciristov et al.,
914 2018), they may represent a plausible mechanism underlying the low-dose and non-
915 monotonic transcriptional responses we observed in this study (Vandenberg et al.,
916 2012).

917 Our findings suggest that plastic-derived chemicals may influence developmental
918 regulation in *Montipora capitata*, potentially via endocrine-like cellular signaling
919 pathways. Although cnidarians do not possess discrete endocrine organs comparable
920 to those found in vertebrates, several components of steroid signaling pathways have
921 been identified in corals and other anthozoans (A. M. Tarrant, 2005; Ann M. Tarrant,
922 2007). In vertebrates, reproductive development and gametogenesis are coordinated
923 through endocrine signaling networks in which hormones bind receptor proteins that
924 regulate downstream gene transcription, and disruption of these pathways by exoge-
925 nous chemicals can alter developmental timing and physiology (McLachlan, 2001).
926 Comparable endocrine-like signaling mechanisms may also occur in corals. Steroid hor-
927 mones including estradiol and estrone have been detected in scleractinian coral tissues,
928 including *Montipora capitata* (A. M. Tarrant et al., 1999), and concentrations of these
929 compounds fluctuate seasonally prior to spawning events (Atkinson & Atkinson, 1992;
930 Slattery et al., 1999; Twan et al., 2006), suggesting that steroid-associated signaling
931 may play a role in coordinating reproductive or developmental processes. In addition,
932 both hard and soft corals are capable of steroid metabolism (Ann M. Tarrant et al.,
933 2003), further supporting the presence of hormonally-responsive biochemical pathways
934 in cnidarians (A. M. Tarrant, 2005).

935 The relatively targeted response we observed contrasts with previous work showing
936 broader transcriptional and developmental disruption following PVC leachate expo-
937 sure. Paganos et al. (2023) reported extensive downregulation of developmental genes
938 in embryos of the sea urchin *Strongylocentrotus purpuratus* exposed to PVC leachates,
939 suggesting impairment of normal developmental progression. Several factors may
940 explain the more limited responses we observed here, including differences in leachate
941 composition, exposure concentration, exposure duration, or species-specific sensitivity.
942 The absence of broad transcriptional disruption in our study further suggests that the
943 environmentally relevant concentrations used here remained below thresholds that
944 cause acute developmental toxicity.

945 Signaling pathways often respond most strongly within narrow concentration ranges,
946 while higher concentrations may lead to receptor saturation, feedback inhibition,
947 pathway desensitization, or suppression of coordinated transcriptional activity. We
948 observed low and moderate PVC leachate levels elicited stronger transcriptional
949 responses than the highest level, consistent with non-monotonic stress responses
950 observed in other developmental systems.

951 Similar patterns have been observed in other marine invertebrates. For example, Xu
952 et al. (2021) found that environmentally relevant concentrations of Di(2-ethylhexyl)
953 phthalate (DEHP), a common plasticizer added to PVC, produced biphasic responses
954 in antioxidant activity and energy metabolism in *Mytilus galloprovincialis*, including
955 U-shaped and inverted U-shaped dose-response relationships. Together, these find-
956 ings indicate that sublethal exposure of coral embryos to plastic leachate can alter

957 developmental signaling in a non-dose dependent manner, and this mechanism may be
958 mediated by G-protein coupled receptors.

959 **4.3 H₃: PVC leachate exposure produced targeted and non-linear shifts** 960 **in a limited subset of bacterial taxa and may alter the functional** 961 **potential of the embryonic coral microbiome**

962 Corals are holobiont organisms that depend on dynamic interactions with their
963 associated microbial communities to support nutrient cycling, immune defense,
964 and host health. In our study, embryonic microbiome composition was shaped by
965 developmental progression rather than by PVC leachate exposure, consistent with
966 previous work showing that bacterial communities in *Montipora capitata* shift during
967 embryogenesis, metamorphosis, and settlement (Bernasconi et al., 2019; Huffmyer et
968 al., 2025).

969 Coral embryo microbiome studies are still an emerging field, with foundational work
970 on early-life-stage coral microbiomes only beginning in the 2010s (Apprill et al., 2012).
971 (Apprill et al., 2012) were among the first to characterize coral embryos (*Pocillopora*
972 *meandrina*) bacterial specificity during development. To our knowledge, our study
973 appears to be the first to characterize the microbiome of coral embryos exposed to
974 plasticizers.

975 Although PVC leachate did not cause broad restructuring of the embryo-associated
976 microbiome, we found shifts in abundance and prevalence of specific bacterial taxa
977 in response to treatment. In particular, the *Methylophaga Marine Methylophagic*
978 *Group 3* increased in abundance and prevalence models across all PVC leachate levels
979 compared to the FSW control. Studies of early coral microbiome establishment consistently
980 show that embryos and early larvae carry highly dynamic, diverse, and largely
981 transient bacterial communities dominated by Proteobacteria. Endozoicomadaeae,
982 Rhodobacteraceae, and *Methylophaga* (Apprill et al., 2012; Bernasconi et al., 2019).

983 *Methylophaga* are important to coral physiology because they occupy a specialized
984 role in the coral sulfur cycle by consuming dimethylsulfide (DMS), a major break-
985 down product of dimethylsulfoniopropionate (DMSP), which is produced in large
986 quantities by corals and their symbiotic algae (Raina et al., 2010, 2013). DMSP and
987 its downstream products contribute to antioxidant defense, stress signaling, and
988 antimicrobial activity within the coral holobiont, making sulfur cycling central to
989 coral health and microbiome organization (Aguilar et al., 2017; Deschaseaux et al.,
990 2014; Gardner et al., 2017; Jackson et al., 2020). Unlike common coral-associated bac-
991 teria, *Methylophaga* are obligate marine methylotrophs that specialize in using DMS
992 and other one-carbon compounds as energy sources, effectively acting as a sink for
993 sulfur-derived metabolites (Janvier & Grimont, 1995; H. G. Kim et al., 2007; Kröber
994 & Schäfer, 2019; Neufeld et al., 2007). Their enrichment under PVC leachate exposure
995 therefore suggests either direct utilization of plastic-derived methylated compounds or
996 disruption of normal coral sulfur metabolism that alters DMSP/DMS release patterns.
997 Whichever mechanism is operating, the functional implication for coral physiology is
998 similar: a bloom of *Methylophaga* in or around coral embryos would accelerate the
999 consumption of DMS (and possibly methanethiol) in the embryo's immediate chemical
1000 environment. Because DMS itself has antioxidant properties and is part of the broader
1001 stress-response chemistry of corals, removal of DMS by a methylotrophic bloom could
1002 deplete a potential chemical defense in coral embryos. DMS is also an important
1003 atmospheric compound for cloud condensation nuclei implicated in localized cooling,
1004 and it's cycling - entirely mediated by bacteria - impacts regional weather (Fischer &
1005 Jones, 2012; Reisch et al., 2011).

1006 Predicted functional profiling of these responsive taxa further indicated that PVC
1007 leachate exposure may selectively favor microbes with traits related to methanogenesis
1008 and the catabolism of aromatic hydrocarbons and chlorinated compounds. These
1009 functional shifts are consistent with the chemical composition of PVC leachate,

1010 which contains complex dissolved organic carbon mixtures including plasticizers,
1011 aromatic compounds, and chlorinated constituents that can serve as substrates for
1012 specialized marine heterotrophs. Similar stress-associated metabolic restructuring has
1013 been observed in experimentally disturbed coral microbiomes, where environmental
1014 stressors altered microbial metabolism toward increased sulfur and nitrogen cycling,
1015 virulence, and secondary metabolism (Vega Thurber et al., 2009). In this context, the
1016 enrichment of methanogenesis-associated pathways may reflect a dysbiotic microbial
1017 response to chemical stress rather than a stable component of the healthy embryo
1018 microbiome, supporting the broader concept that relatively small shifts in micro-
1019 bial community composition can substantially alter coral holobiont function (Vega
1020 Thurber et al., 2009).

1021 The enrichment of pathways related to aromatic hydrocarbon and chlorinated com-
1022 pound degradation is likewise biologically plausible under PVC exposure. Corals
1023 living near natural hydrocarbon seeps harbor microbial communities enriched in
1024 hydrocarbon-degrading Gammaproteobacteria, Actinobacteria, and Firmicutes capable
1025 of metabolizing compounds such as phenanthrene, biphenyl, and naphthalene, with
1026 degradative capacity increasing alongside contaminant exposure (Al-Dahash & Mah-
1027 moud, 2013). Similarly, coral-associated hydrocarbon-degrading bacteria possess genes
1028 involved not only in aromatic and alkane degradation, but also DMSP metabolism,
1029 nitrogen cycling, cobalamin biosynthesis, and antimicrobial compound production, in-
1030 dicating that these microbes can simultaneously participate in xenobiotic degradation
1031 and holobiont-associated functions (Villela et al., 2023). Because marine organisms
1032 naturally produce halogenated organic compounds, reef-associated bacteria also
1033 commonly encode dehalogenation pathways that participate in the natural marine
1034 chlorine cycle (Atashgahi et al., 2018). However, under PVC leachate exposure,
1035 enrichment of these pathways likely reflects microbial selection for taxa capable of
1036 tolerating or metabolizing plastic-derived aromatic and chlorinated compounds.

1037 These functional predictions should nevertheless be interpreted cautiously, as
1038 PICRUSt-based inference from 16S rRNA data depends strongly on reference genome
1039 representation, which remains limited for many coral-associated marine microbes.
1040 While these traits were inferred from amplicon sequence variant (ASV) phylogenetic
1041 placement rather than direct metagenomic or proteomic measurements (Douglas et al.,
1042 2020), the results suggest that PVC leachate pollution may influence not only which
1043 microbes associate with developing coral embryos, but also the broader metabolic
1044 potential of the embryo-associated microbiome.

1045 These findings are broadly compatible with previous marine microbiome studies
1046 examining PVC leachate exposure in seawater. (Focardi et al., 2022) found that
1047 PVC leachate alone dramatically restructured a natural planktonic marine microbial
1048 community, suppressing primary producers (including SAR11 and picophytoplankton)
1049 while favoring fast-growing copiotrophs in the Alteromonadales. Accompanying
1050 metagenomics showed enrichment in genes for pathogenicity and motility. Related
1051 work by (Vlaanderen et al., 2023) showed that PVC leachate enriches antibiotic-
1052 resistant genes and virulence genes in seawater communities. Although neither study
1053 highlights *Methylophaga*, or is specific to coral, both support the idea that PVC
1054 leachate can affect the microbial environment in the seawater surrounding corals and
1055 their developing embryos.

1056 Together, these results suggest that environmentally relevant PVC exposure may exert
1057 subtle but ecologically meaningful selective pressures on microbial assembly during
1058 coral embryogenesis, even when overall community structure remains relatively stable.

1059 5 Conclusion

1060 At the surface, *Montipora capitata* coral embryos appear largely resilient to PVC
1061 leachate stress, yet we detected several subtle but important biological responses to

1062 PVC leachate pollution. Leachate exposure was associated with small, stage-specific
1063 shifts in developmental timing, suggesting that key embryonic transitions may be
1064 modestly accelerated by PVC leachate exposure. At the molecular level, 130 genes
1065 responded to leachate exposure, indicating targeted transcriptional effects nested
1066 within broader embryonic regulation. Similarly, the embryo-associated microbiome
1067 did not undergo large community-wide restructuring, yet specific bacterial taxa (and
1068 subsequently their predicted functional pathways) were impacted by PVC leachate
1069 exposure, particularly those linked to aromatic carbon degradation and DMSP cycling.
1070 Together, these findings suggest that PVC leachate may exert hidden sublethal effects
1071 that are not captured by traditional survival-based endpoints.

1072 These findings reveal that exposure to plastic-derived chemicals can subtly alter devel-
1073 opment, gene regulation, and host-associated microbiomes during the most sensitive
1074 stages of coral life history. Such early, low-dose effects may scale up to influence larval
1075 performance, recruitment success, and ultimately coral population resilience. The
1076 patterns detected here are consistent with the expected effects of endocrine-disrupting
1077 chemicals operating through low-dose, endocrine-like signaling.

1078 Future studies should investigate whether acute early-life exposure to PVC leachate
1079 produces longer-term consequences that persist beyond embryogenesis, including
1080 effects on epigenetic regulation, larval survival trajectories, metamorphosis, and
1081 settlement success. Because this study focused on acute exposure, additional work
1082 examining chronic or repeated exposure scenarios is also needed to better reflect
1083 environmentally realistic conditions. Plastic pollution rarely occurs in isolation
1084 in reef environments, and future experiments should therefore examine how PVC
1085 leachate interacts with additional stressors such as thermal stress from ocean warming
1086 and marine heatwaves. Furthermore, PVC leachate represents only one subset of
1087 microplastic polymers and associated additive chemicals, and substantially more work
1088 is needed to characterize the toxicity of other plastic types and chemical mixtures.

1089 This study is relevant to the conservation and management of coral reef ecosystems,
1090 and can inform conservation, management, and policy decisions on plastics and their
1091 chemical additives as emerging contaminants of concern. Support for regulations that
1092 recognize and mitigate the impacts of low-dose endocrine-disrupting chemicals on
1093 vulnerable marine ecosystems is critical for protecting these vital life-giving resources
1094 (Vandenberg, 2021).

1095 **6 Acknowledgements**

1096 This experiment was conducted on Oahu, Hawai i. As guests, we recognize and give
1097 thanks for the land and water resources of the aina and the traditional owners of the
1098 land, kanaka oiwi, both past and present, as well as future generations, on which
1099 this experimental work was conducted in the Kane ohe Ahupua a. Molecular lab
1100 work and computational analysis were conducted in Seattle, WA. We therefore wish
1101 to acknowledge the Coast Salish peoples of the land that touches the shared waters
1102 of all tribes and bands within the Suquamish, Tulalip, and Muckleshoot nations.
1103 We are grateful for the logistical support provided by the Donohue Lab, the Coral
1104 Resilience Lab and the Hawai i Institute of Marine Biology. We acknowledge use of
1105 the computational resources of the Roberts Lab, and have immense gratitude for the
1106 guidance of Sam White and Ariana Huffmyer. We acknowledge coral colony collection
1107 by Callum Backstrom and Katherine Lasdin, as well as experimental assay setup and
1108 sample collection by Katherine Lasdin. We acknowledge Savannah Leidholdt, Jesse
1109 Zaneveld, and Amy Van Cise for helpful discussions on 16S bacterial analyses.

1110 **7 Competing interests**

1111 The authors declare that they have no known competing financial interests or personal
1112 relationships that could have appeared to influence the work reported in this paper.

1113 **8 Author contributions**

1114 S.T. conducted the investigation, developed the methodology, performed formal
 1115 analyses, administered the project, created visualizations, and wrote the original
 1116 draft of the manuscript. S.R. provided supervision and resources and contributed to
 1117 writing, review, and editing. F.S. provided resources, contributed to validation, and
 1118 participated in writing, review, and editing. S.S. provided resources, contributed to
 1119 formal analysis, and participated in writing, review, and editing. J.L.P.G. conceived
 1120 the study, acquired funding, supervised the project, and contributed to writing the
 1121 original draft of the manuscript.

1122 **9 Funding**

1123 This research was supported by the National Science Foundation CAREER Grant
 1124 (award no.), the University of Washington College of Environment Benjamin and
 1125 Margaret Hall Student Research Support Fund , and the University of Washington
 1126 School of Aquatic & Fishery Sciences Finishing Fellowship.

1127 **10 Data availability**

1128 Raw paired-end reads (FASTQ format) of RNA-Seq and 16S were deposited and
 1129 are publicly available in the National Center for Biotechnology Information (NCBI)
 1130 Sequence Read Archive (SRA) under BioProject accession numbers PRJNA1177827
 1131 and PRJNA1244351.

1132 **11 AI**

1133 **Declaration of generative AI and AI-assisted technologies in the manuscript**
 1134 **preparation process**

1135 During the preparation of this work the author(s) used ChatGPT in order to sum-
 1136 marize methods of analysis in R, and Elicit to search for peer reviewed papers. After
 1137 using this tool/service, the author(s) reviewed and edited the content as needed and
 1138 take(s) full responsibility for the content of the published article.

1139 **12 Supplementary**

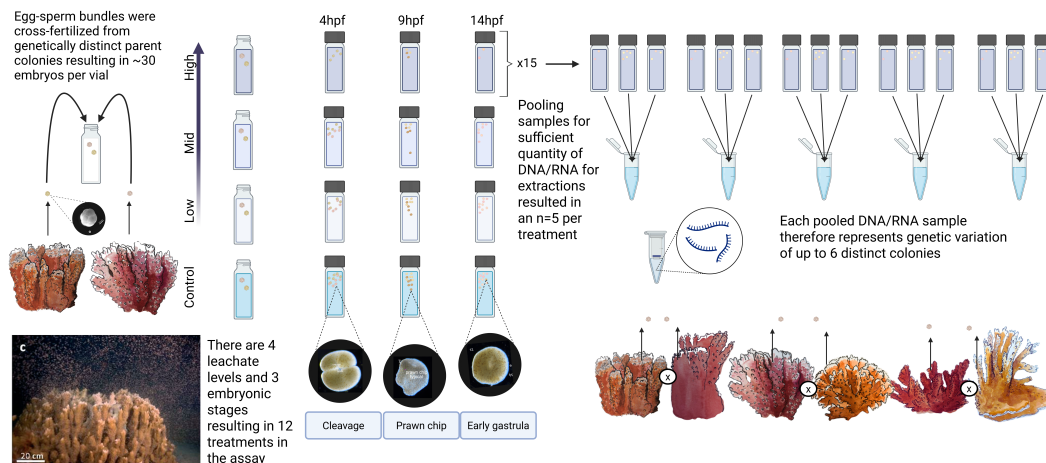


Figure 16: Experimental overview of *Montipora capitata* early life-stage exposure to PVC leachate. Schematic showing the reproductive biology and experimental design used to obtain coral embryos and assess the effects of plastic-derived leachates during early development.

Table 1: Summary of embryo count means indicating survival of embryos across treatment and developmental time

Hours post-fertilization	Control (FSW)	Low (0.01 mg/L)	Mid (0.1 mg/L)	High (1 mg/L)
4	27.0 ± 3.9	27.3 ± 4.9	24.0 ± 5.4	26.0 ± 3.2
9	12.4 ± 7.5	12.6 ± 8.8	12.9 ± 6.1	11.1 ± 8.0
14	11.3 ± 5.6	12.7 ± 4.7	14.2 ± 7.2	9.6 ± 4.6

Table 2: ANOVA results for relative survival of embryos across treatment and developmental time

Term	df	Sum Sq	Mean Sq	F value	Pr(>F)
PVC leachate treatment	3	57.51852	19.17284	0.5228956	0.6675647
Developmental stage (hpf)	2	4696.35185	2348.17593	64.0411616	0.0000000
Treatment × stage	6	125.87037	20.97840	0.5721380	0.7516086
Residuals	96	3520.00000	36.66667	NA	NA

Table 3: Multivariate and univariate results of embryo developmental timing stage composition

Effect	Df	De-		p-		Dev		p		Dev		p	
		viance	value	Dev	p	Dev	p	Dev	p	Dev	p		
Treatment	3	1.50	0.998	0.14	0.999	0.52	0.999	0.36	0.999	0.03	0.999	0.46	0.999
hpf	2	568.00	0.001**	111.980	0.001**	76.46	0.001**	71.99	0.001**	126.170	0.001**	181.390	0.001**
Treatment × hpf	6	40.30	0.009**	16.53	0.108	2.76	0.144	9.42	0.108	11.59	0.108	0.00	0.791

Table 4: Multivariate and univariate results of embryo morphological abnormality status

Effect	Df	De-		p-		Dev		p		Dev		p	
		viance	p-value	Dev	p	Dev	p	Dev	p	Dev	p		
Treatment	3	5.47	0.701	0.37	0.949	0.86	0.949	4.24	0.470				
hpf	2	90.91	0.001**	63.75	0.001**	25.24	0.001**	1.91	0.387				
Treatment × hpf	6	12.12	0.886	4.69	0.870	6.14	0.854	1.29	0.982				

- 1140 Aguilar, C., Raina, J.-B., Motti, C. A., Fôret, S., Hayward, D. C., Lapeyre, B., et
 1141 al. (2017). Transcriptomic analysis of the response of acropora millepora to
 1142 hypo-osmotic stress provides insights into DMSP biosynthesis by corals. *BMC*
 1143 *Genomics*, 18, 612. <https://doi.org/10.1186/s12864-017-3959-0>
 1144 Al-Dahash, L. M., & Mahmoud, H. M. (2013). Harboring oil-degrading bacteria:
 1145 A potential mechanism of adaptation and survival in corals inhabiting oil-
 1146 contaminated reefs. *Marine Pollution Bulletin*, 72, 364–374. [https://doi.org/](https://doi.org/10.1016/j.marpolbul.2012.08.029)
 1147 [10.1016/j.marpolbul.2012.08.029](https://doi.org/10.1016/j.marpolbul.2012.08.029)

- 1148 Anselmo, H. M. R., Koerting, L., Devito, S., Berg, J. H. J. van den, Dubbeldam, M.,
 1149 Kwadijk, C., & Murk, A. J. (2011). Early life developmental effects of marine
 1150 persistent organic pollutants on the sea urchin *psammechinus miliaris*. *Ecotox-*
 1151 *icology and Environmental Safety*, *74*, 2182–2192. [https://doi.org/10.1016/](https://doi.org/10.1016/j.ecoenv.2011.07.037)
 1152 [j.ecoenv.2011.07.037](https://doi.org/10.1016/j.ecoenv.2011.07.037)
- 1153 Apprill, A., Marlow, H. Q., Martindale, M. Q., & Rappé, M. S. (2012). Specificity
 1154 of associations between bacteria and the coral pocillopora meandrina during
 1155 early development. *Applied and Environmental Microbiology*, *78*, 7467–7475.
 1156 <https://doi.org/10.1128/AEM.01232-12>
- 1157 Atashgahi, S., Liebensteiner, M. G., Janssen, D. B., Smidt, H., Stams, A. J.
 1158 M., & Sipkema, D. (2018). Microbial synthesis and transformation of inor-
 1159 ganic and organic chlorine compounds. *Frontiers in Microbiology*, *9*, 3079.
 1160 <https://doi.org/10.3389/fmicb.2018.03079>
- 1161 Atkinson, S., & Atkinson, M. J. (1992). Detection of estradiol-17 β During a mass
 1162 coral spawn. *Coral Reefs*, *11*, 33–35. <https://doi.org/10.1007/bf00291932>
- 1163 Bernasconi, R., Stat, M., Koenders, A., Papparini, A., Bunce, M., & Huggett, M.
 1164 J. (2019). Establishment of coral-bacteria symbioses reveal changes in the core
 1165 bacterial community with host ontogeny. *Frontiers in Microbiology*, *10*, 1529.
 1166 <https://doi.org/10.3389/fmicb.2019.01529>
- 1167 Berry, K. L. E., Epstein, H. E., Lewis, P. J., Hall, N. M., & Negri, A. P. (2019).
 1168 Microplastic contamination has limited effects on coral fertilisation and larvae.
 1169 *Diversity*, *11*, 228. <https://doi.org/10.3390/d11120228>
- 1170 Bolyen, E., Rideout, J. R., Dillon, M. R., Bokulich, N. A., Abnet, C. C., Al-Ghalith,
 1171 G. A., et al. (2019). Reproducible, interactive, scalable and extensible mi-
 1172 crobiome data science using QIIME 2. *Nature Biotechnology*, *37*, 852–857.
 1173 <https://doi.org/10.1038/s41587-019-0209-9>
- 1174 Capolupo, M., Rafiq, A., Coralli, I., Alessandro, T., Valbonesi, P., Fabbri, D.,
 1175 & Fabbri, E. (2023). Bioplastic leachates characterization and impacts on
 1176 early larval stages and adult mussel cellular, biochemical and physiological
 1177 responses. *Environmental Pollution (Barking, Essex: 1987)*, *319*, 120951.
 1178 <https://doi.org/10.1016/j.envpol.2022.120951>
- 1179 Chen, S. (2023). Ultrafast one-pass FASTQ data preprocessing, quality control, and
 1180 deduplication using fastp. *iMeta*, *2*, e107. <https://doi.org/10.1002/imt2.107>
- 1181 Chille, E., Strand, E., Neder, M., Schmidt, V., Sherman, M., Mass, T., & Putnam,
 1182 H. (2021). Developmental series of gene expression clarifies maternal mRNA
 1183 provisioning and maternal-to-zygotic transition in a reef-building coral. *BMC*
 1184 *Genomics*, *22*, 815. <https://doi.org/10.1186/s12864-021-08114-y>
- 1185 Chille, E. E., Strand, E. L., Scucchia, F., Neder, M., Schmidt, V., Sherman, M. O., et
 1186 al. (2022). Energetics, but not development, is impacted in coral embryos exposed
 1187 to ocean acidification. *The Journal of Experimental Biology*, *225*, jeb243187.
 1188 <https://doi.org/10.1242/jeb.243187>
- 1189 Civciristov, S., Ellisdon, A. M., Suderman, R., Pon, C. K., Evans, B. A., Kleifeld, O.,
 1190 et al. (2018). Preassembled GPCR signaling complexes mediate distinct cellular
 1191 responses to ultralow ligand concentrations. *Science Signaling*, *11*, ean1188.
 1192 <https://doi.org/10.1126/scisignal.aan1188>
- 1193 Claar, D. C., Starko, S., Tietjen, K. L., Epstein, H. E., Cunning, R., Cobb, K. M.,
 1194 et al. (2020). Dynamic symbioses reveal pathways to coral survival through
 1195 prolonged heatwaves. *Nature Communications*, *11*, 6097. [https://doi.org/](https://doi.org/10.1038/s41467-020-19169-y)
 1196 [10.1038/s41467-020-19169-y](https://doi.org/10.1038/s41467-020-19169-y)
- 1197 Danecek, P., Bonfield, J. K., Liddle, J., Marshall, J., Ohan, V., Pollard, M. O.,
 1198 et al. (2021). Twelve years of SAMtools and BCFtools. *GigaScience*, *10*.
 1199 <https://doi.org/10.1093/gigascience/giab008>
- 1200 Deschaseaux, E. S. M., Jones, G. B., Deseo, M. A., Shepherd, K. M., Kiene, R. P.,
 1201 Swan, H. B., et al. (2014). Effects of environmental factors on dimethylated sulfur
 1202 compounds and their potential role in the antioxidant system of the coral holo-

- 1203 biont. *Limnology and Oceanography*, 59, 758–768. <https://doi.org/10.4319/>
 1204 [lo.2014.59.3.0758](https://doi.org/10.4319/lo.2014.59.3.0758)
- 1205 Douglas, G. M., Maffei, V. J., Zaneveld, J. R., Yurgel, S. N., Brown, J. R., Taylor,
 1206 C. M., et al. (2020). PICRUSt2 for prediction of metagenome functions. *Nature*
 1207 *Biotechnology*, 38, 685–688. <https://doi.org/10.1038/s41587-020-0548-6>
- 1208 Eddy, T. D., Cheung, W. W. L., & Bruno, J. F. (2018). Historical baselines of
 1209 coral cover on tropical reefs as estimated by expert opinion. *PeerJ*, 6, e4308.
 1210 <https://doi.org/10.7717/peerj.4308>
- 1211 Eddy, T. D., Lam, V. W. Y., Reygondeau, G., Cisneros-Montemayor, A. M., Greer,
 1212 K., Palomares, M. L. D., et al. (2021). Global decline in capacity of coral reefs
 1213 to provide ecosystem services. *One Earth (Cambridge, Mass.)*, 4, 1278–1285.
 1214 <https://doi.org/10.1016/j.oneear.2021.08.016>
- 1215 Ewels, P., Magnusson, M., Lundin, S., & Källers, M. (2016). MultiQC: Summarize
 1216 analysis results for multiple tools and samples in a single report. *Bioinformatics*
 1217 *(Oxford, England)*, 32, 3047–3048. [https://doi.org/10.1093/bioinformatics/](https://doi.org/10.1093/bioinformatics/btw354)
 1218 [btw354](https://doi.org/10.1093/bioinformatics/btw354)
- 1219 Fischer, E., & Jones, G. (2012). Atmospheric dimethylsulphide production from corals
 1220 in the great barrier reef and links to solar radiation, climate and coral bleaching.
 1221 *Biogeochemistry*, 110, 31–46. <https://doi.org/10.1007/s10533-012-9719-y>
- 1222 Focardi, A., Moore, L. R., Raina, J.-B., Seymour, J. R., Paulsen, I. T., & Tetu,
 1223 S. G. (2022). Plastic leachates impair picophytoplankton and dramatically re-
 1224 shape the marine microbiome. *Microbiome*, 10, 179. [https://doi.org/10.1186/](https://doi.org/10.1186/s40168-022-01369-x)
 1225 [s40168-022-01369-x](https://doi.org/10.1186/s40168-022-01369-x)
- 1226 Gambardella, C., Miroglio, R., Prieto Amador, M., Castelli, F., Castellano, L., Piazza,
 1227 V., et al. (2024). High concentrations of phthalates affect the early development of
 1228 the sea urchin *paracentrotus lividus*. *Ecotoxicology and Environmental Safety*, 279,
 1229 116473. <https://doi.org/10.1016/j.ecoenv.2024.116473>
- 1230 Gardner, S. G., Raina, J.-B., Nitschke, M. R., Nielsen, D. A., Stat, M., Motti, C.
 1231 A., et al. (2017). A multi-trait systems approach reveals a response cascade
 1232 to bleaching in corals. *BMC Biology*, 15, 117. [https://doi.org/10.1186/](https://doi.org/10.1186/s12915-017-0459-2)
 1233 [s12915-017-0459-2](https://doi.org/10.1186/s12915-017-0459-2)
- 1234 Gloor, G. B., Macklaim, J. M., Pawlowsky-Glahn, V., & Egozcue, J. J. (2017).
 1235 Microbiome datasets are compositional: And this is not optional. *Frontiers in*
 1236 *Microbiology*, 8, 2224. <https://doi.org/10.3389/fmicb.2017.02224>
- 1237 Grasso, L. C., Hayward, D. C., Trueman, J. W., Hardie, K. M., Janssens, P. A., &
 1238 Ball, E. E. (2001). The evolution of nuclear receptors: Evidence from the coral
 1239 acropora. *Molecular Phylogenetics and Evolution*, 21, 93–102. [https://doi.org/](https://doi.org/10.1006/mpev.2001.0994)
 1240 [10.1006/mpev.2001.0994](https://doi.org/10.1006/mpev.2001.0994)
- 1241 Grasso, Lauretta C., Maindonald, J., Rudd, S., Hayward, D. C., Saint, R., Miller, D.
 1242 J., & Ball, E. E. (2008). Microarray analysis identifies candidate genes for key
 1243 roles in coral development. *BMC Genomics*, 9, 540. [https://doi.org/10.1186/](https://doi.org/10.1186/1471-2164-9-540)
 1244 [1471-2164-9-540](https://doi.org/10.1186/1471-2164-9-540)
- 1245 Gunaalan, K., Fabbri, E., & Capolupo, M. (2020). The hidden threat of plastic
 1246 leachates: A critical review on their impacts on aquatic organisms. *Water Re-*
 1247 *search*, 184, 116170. <https://doi.org/10.1016/j.watres.2020.116170>
- 1248 Hahladakis, J. N., Velis, C. A., Weber, R., Iacovidou, E., & Purnell, P. (2018). An
 1249 overview of chemical additives present in plastics: Migration, release, fate and envi-
 1250 ronmental impact during their use, disposal and recycling. *Journal of Hazardous*
 1251 *Materials*, 344, 179–199. <https://doi.org/10.1016/j.jhazmat.2017.10.014>
- 1252 Hambleton, E., Jones, V. A. S., Maegele, I., Vaskoff, D., Sachsenheimer, T., & Guse,
 1253 A. (2018). Enhanced stability of non-canonical NPC2 in the symbiosome supports
 1254 coral-algal symbiosis. *bioRxiv*, 399766. <https://doi.org/10.1101/399766>
- 1255 Hermabessiere, L., Dehaut, A., Paul-Pont, I., Lacroix, C., Jezequel, R., Soudant,
 1256 P., & Duflos, G. (2022). Occurrence and effects of plastic additives on ma-

- 1257 rine environments and organisms: A review. *Chemosphere*, *182*, 781–793.
 1258 <https://doi.org/10.1016/j.chemosphere.2017.05.096>
- 1259 Heyward, A. J., & Negri, A. P. (2012). Turbulence, cleavage, and the naked embryo:
 1260 A case for coral clones. *Science (New York, N.Y.)*, *335*, 1064. [https://doi.org/](https://doi.org/10.1126/science.1216055)
 1261 [10.1126/science.1216055](https://doi.org/10.1126/science.1216055)
- 1262 Huffmyer, A. S., Wong, K. H., Becker, D. M., Strand, E., Mass, T., & Putnam, H.
 1263 M. (2023). Multi-omic analysis of coral development elucidates the metabolic
 1264 transitions from parental provisioning to endosymbiotic nutritional exchange.
 1265 *bioRxiv*. <https://doi.org/10.1101/2023.03.20.533475>
- 1266 Huffmyer, A. S., Wong, K. H., Becker, D. M., Strand, E., Mass, T., & Putnam,
 1267 H. M. (2025). Shifts and critical periods in coral metabolism reveal ener-
 1268 getic vulnerability during development. *Current Biology*, *35*, 2858–2871.e6.
 1269 <https://doi.org/10.1016/j.cub.2025.05.013>
- 1270 Isa, V., Seveso, D., Diamante, L., Montalbetti, E., Montano, S., Gobbato, J., et al.
 1271 (2024). Physical and cellular impact of environmentally relevant microplastic
 1272 exposure on thermally challenged pocillopora damicornis (cnidaria, scleractinia).
 1273 *The Science of the Total Environment*, *918*, 170651. [https://doi.org/10.1016/](https://doi.org/10.1016/j.scitotenv.2024.170651)
 1274 [j.scitotenv.2024.170651](https://doi.org/10.1016/j.scitotenv.2024.170651)
- 1275 Isa, V., Saliu, F., Becchi, A., Spadaccino, G., Quinto, M., Veronelli, M., et al. (2025).
 1276 Impacts of microplastics on reef-building corals: Disentangling the contribution of
 1277 the chain scission products released by weathering. *The Science of the Total Envi-*
 1278 *ronment*, *975*, 179239. <https://doi.org/10.1016/j.scitotenv.2025.179239>
- 1279 Jackson, R. L., Gabric, A. J., Cropp, R., & Woodhouse, M. T. (2020). Dimethyl-
 1280 sulfide (DMS), marine biogenic aerosols and the ecophysiology of coral reefs.
 1281 *Biogeosciences*, *17*, 2181–2204. <https://doi.org/10.5194/bg-17-2181-2020>
- 1282 Jambeck, J. R., Geyer, R., Wilcox, C., Siegler, T. R., Perryman, M., Andrady,
 1283 A., et al. (2015). Marine pollution. Plastic waste inputs from land into the
 1284 ocean. *Science (New York, N.Y.)*, *347*, 768–771. [https://doi.org/10.1126/](https://doi.org/10.1126/science.1260352)
 1285 [science.1260352](https://doi.org/10.1126/science.1260352)
- 1286 Janvier, M., & Grimont, P. A. (1995). The genus methylophaga, a new line of descent
 1287 within phylogenetic branch gamma of proteobacteria. *Research in Microbiology*,
 1288 *146*, 543–550. [https://doi.org/10.1016/0923-2508\(96\)80560-2](https://doi.org/10.1016/0923-2508(96)80560-2)
- 1289 Jimenez-Guri, E., Murano, C., Paganos, P., & Arnone, M. I. (2023). PVC pellet
 1290 leachates affect adult immune system and embryonic development but not repro-
 1291 ductive capacity in the sea urchin *paracentrotus lividus*. *Marine Pollution Bulletin*,
 1292 *196*, 115604. <https://doi.org/10.1016/j.marpolbul.2023.115604>
- 1293 Kim, D., Paggi, J. M., Park, C., Bennett, C., & Salzberg, S. L. (2019). Graph-based
 1294 genome alignment and genotyping with HISAT2 and HISAT-genotype. *Nature*
 1295 *Biotechnology*, *37*, 907–915. <https://doi.org/10.1038/s41587-019-0201-4>
- 1296 Kim, H. G., Doronina, N. V., Trotsenko, Y. A., & Kim, S. W. (2007). Methylophaga
 1297 aminisulfidivorans sp. Nov., a restricted facultatively methylotrophic marine
 1298 bacterium. *International Journal of Systematic and Evolutionary Microbiology*, *57*,
 1299 2096–2101. <https://doi.org/10.1099/ijs.0.65139-0>
- 1300 Kröber, E., & Schäfer, H. (2019). Identification of proteins and genes expressed
 1301 by methylophaga thiooxydans during growth on dimethylsulfide and their
 1302 presence in other members of the genus. *Frontiers in Microbiology*, *10*, 1132.
 1303 <https://doi.org/10.3389/fmicb.2019.01132>
- 1304 Lamb, J. B., Willis, B. L., Fiorenza, E. A., Couch, C. S., Howard, R., Rader, D. N., et
 1305 al. (2018). Plastic waste associated with disease on coral reefs. *Science (New York,*
 1306 *N.Y.)*, *359*, 460–462. <https://doi.org/10.1126/science.aar3320>
- 1307 Langfelder, P., & Horvath, S. (2008). WGCNA: An R package for weighted correla-
 1308 tion network analysis. *BMC Bioinformatics*, *9*, 559. [https://doi.org/10.1186/](https://doi.org/10.1186/1471-2105-9-559)
 1309 [1471-2105-9-559](https://doi.org/10.1186/1471-2105-9-559)
- 1310 Law, R. J., Fileman, T. W., & Matthiessen, P. (1991). Phthalate esters and other
 1311 industrial organic chemicals in the north and irish seas. *Water Science and Tech-*

- 1312 *nology: A Journal of the International Association on Water Pollution Research*,
 1313 *24*, 127–134. <https://doi.org/10.2166/wst.1991.0283>
- 1314 Love, M. I., Huber, W., & Anders, S. (2014). Moderated estimation of fold change
 1315 and dispersion for RNA-seq data with DESeq2. *Genome Biology*, *15*, 550.
 1316 <https://doi.org/10.1186/s13059-014-0550-8>
- 1317 Lynch, J. M., Knauer, K., & Shaw, K. R. (2022, April 20). Plastic additives
 1318 in the ocean. (A. L. Andrady, Ed.). Wiley. [https://doi.org/10.1002/](https://doi.org/10.1002/9781119768432.ch2)
 1319 [9781119768432.ch2](https://doi.org/10.1002/9781119768432.ch2)
- 1320 MacLeod, M., Arp, H. P. H., Tekman, M. B., & Jahnke, A. (2021). The global threat
 1321 from plastic pollution. *Science (New York, N.Y.)*, *373*, 61–65. [https://doi.org/](https://doi.org/10.1126/science.abg5433)
 1322 [10.1126/science.abg5433](https://doi.org/10.1126/science.abg5433)
- 1323 Mallick, H., Rahnavard, A., McIver, L. J., Ma, S., Zhang, Y., Nguyen, L. H., et
 1324 al. (2021). Multivariable association discovery in population-scale meta-omics
 1325 studies. *PLoS Computational Biology*, *17*, e1009442. [https://doi.org/10.1371/](https://doi.org/10.1371/journal.pcbi.1009442)
 1326 [journal.pcbi.1009442](https://doi.org/10.1371/journal.pcbi.1009442)
- 1327 Maqbool, F., Mostafalou, S., Bahadar, H., & Abdollahi, M. (2016). Review of
 1328 endocrine disorders associated with environmental toxicants and possible in-
 1329 volved mechanisms. *Life Sciences*, *145*, 265–273. [https://doi.org/10.1016/](https://doi.org/10.1016/j.lfs.2015.10.022)
 1330 [j.lfs.2015.10.022](https://doi.org/10.1016/j.lfs.2015.10.022)
- 1331 Mathieu, C., & Bednarek, J. (2022). *Survey of phthalates in washington state*
 1332 *waterbodies, 2021* (research report No. 22-03-027). Washington State Depart-
 1333 ment of Ecology, Olympia. Retrieved from [https://apps.ecology.wa.gov/](https://apps.ecology.wa.gov/publications/documents/2203027.pdf)
 1334 [publications/documents/2203027.pdf](https://apps.ecology.wa.gov/publications/documents/2203027.pdf)
- 1335 McLachlan, J. A. (2001). Environmental signaling: What embryos and evolution
 1336 teach us about endocrine disrupting chemicals. *Endocrine Reviews*, *22*, 319–341.
 1337 <https://doi.org/10.1210/edrv.22.3.0432>
- 1338 Meijer, L. J. J., Emmerik, T. van, Ent, R. van der, Schmidt, C., & Lebreton, L.
 1339 (2021). More than 1000 rivers account for 80% of global riverine plastic emissions
 1340 into the ocean. *Science Advances*, *7*, eaaz5803. [https://doi.org/10.1126/](https://doi.org/10.1126/sciadv.aaz5803)
 1341 [sciadv.aaz5803](https://doi.org/10.1126/sciadv.aaz5803)
- 1342 Morgan, M. B., Ross, J., Ellwanger, J., Phrommala, R. M., Youngblood, H., Qualley,
 1343 D., & Williams, J. (2022). Sea anemones responding to sex hormones, oxybenzone,
 1344 and benzyl butyl phthalate: Transcriptional profiling and in silico modelling
 1345 provide clues to decipher endocrine disruption in cnidarians. *Frontiers in Ge-*
 1346 *netics*, *12*. Retrieved from [https://www.frontiersin.org/articles/10.3389/](https://www.frontiersin.org/articles/10.3389/fgene.2021.793306)
 1347 [fgene.2021.793306](https://www.frontiersin.org/articles/10.3389/fgene.2021.793306)
- 1348 Net, S., Delmont, A., Sempéré, R., Paluselli, A., & Ouddane, B. (2015). Reliable
 1349 quantification of phthalates in environmental matrices (air, water, sludge, sediment
 1350 and soil): A review. *The Science of the Total Environment*, *515-516*, 162–180.
 1351 <https://doi.org/10.1016/j.scitotenv.2015.02.013>
- 1352 Neufeld, J. D., Schäfer, H., Cox, M. J., Boden, R., McDonald, I. R., & Murrell, J. C.
 1353 (2007). Stable-isotope probing implicates methylphaga spp and novel gammapro-
 1354 teobacteria in marine methanol and methylamine metabolism. *The ISME Journal*,
 1355 *1*, 480–491. <https://doi.org/10.1038/ismej.2007.65>
- 1356 O'Connor, M. I., Bruno, J. F., Gaines, S. D., Halpern, B. S., Lester, S. E., Kinlan,
 1357 B. P., & Weiss, J. M. (2007). Temperature control of larval dispersal and the
 1358 implications for marine ecology, evolution, and conservation. *Proceedings of the*
 1359 *National Academy of Sciences of the United States of America*, *104*, 1266–1271.
 1360 <https://doi.org/10.1073/pnas.0603422104>
- 1361 Okubo, N., Mezaki, T., Nozawa, Y., Nakano, Y., Lien, Y.-T., Fukami, H., et al.
 1362 (2013). Comparative embryology of eleven species of stony corals (scleractinia).
 1363 *PloS One*, *8*, e84115. <https://doi.org/10.1371/journal.pone.0084115>
- 1364 Oppen, M. J. H. van, Gates, R. D., Blackall, L. L., Cantin, N., Chakravarti, L. J.,
 1365 Chan, W. Y., et al. (2017). Shifting paradigms in restoration of the world's

- 1366 coral reefs. *Global Change Biology*, *23*, 3437–3448. [https://doi.org/10.1111/](https://doi.org/10.1111/gcb.13647)
 1367 [gcb.13647](https://doi.org/10.1111/gcb.13647)
- 1368 Padilla-Gamiño, & Gates. (2012). Spawning dynamics in the hawaiian reef-building
 1369 coral montipora capitata. *Marine Ecology Progress Series*, *449*, 145–160.
 1370 <https://doi.org/10.3354/meps09530>
- 1371 Padilla-Gamiño, J. L., Weatherby, T. M., Waller, R. G., & Gates, R. D. (2011). For-
 1372 mation and structural organization of the egg–sperm bundle of the scleractinian
 1373 coral montipora capitata. *Coral Reefs*, *30*, 371–380. [https://doi.org/10.1007/](https://doi.org/10.1007/s00338-010-0700-8)
 1374 [s00338-010-0700-8](https://doi.org/10.1007/s00338-010-0700-8)
- 1375 Paganos, P., Ullmann, C. V., Gaglio, D., Bonanomi, M., Salmistraro, N., Arnone, M.
 1376 I., & Jimenez-Guri, E. (2023). Plastic leachate-induced toxicity during sea urchin
 1377 embryonic development: Insights into the molecular pathways affected by PVC.
 1378 *The Science of the Total Environment*, *864*, 160901. [https://doi.org/10.1016/](https://doi.org/10.1016/j.scitotenv.2022.160901)
 1379 [j.scitotenv.2022.160901](https://doi.org/10.1016/j.scitotenv.2022.160901)
- 1380 Paluselli, A., Fauvelle, V., Schmidt, N., Galgani, F., Net, S., & Sempéré, R. (2018).
 1381 Distribution of phthalates in marseille bay (NW mediterranean sea). *The Sci-*
 1382 *ence of the Total Environment*, *621*, 578–587. [https://doi.org/10.1016/](https://doi.org/10.1016/j.scitotenv.2017.11.306)
 1383 [j.scitotenv.2017.11.306](https://doi.org/10.1016/j.scitotenv.2017.11.306)
- 1384 Perteau, M., Perteau, G. M., Antonescu, C. M., Chang, T.-C., Mendell, J. T., &
 1385 Salzberg, S. L. (2015). StringTie enables improved reconstruction of a transcrip-
 1386 tome from RNA-seq reads. *Nature Biotechnology*, *33*, 290–295. [https://doi.org/](https://doi.org/10.1038/nbt.3122)
 1387 [10.1038/nbt.3122](https://doi.org/10.1038/nbt.3122)
- 1388 Pinheiro, M., Martins, I., Raimundo, J., Caetano, M., Neuparth, T., & Santos,
 1389 M. M. (2023). Stressors of emerging concern in deep-sea environments: Mi-
 1390 croplastics, pharmaceuticals, personal care products and deep-sea mining. *The*
 1391 *Science of the Total Environment*, *876*, 162557. [https://doi.org/10.1016/](https://doi.org/10.1016/j.scitotenv.2023.162557)
 1392 [j.scitotenv.2023.162557](https://doi.org/10.1016/j.scitotenv.2023.162557)
- 1393 Raina, J.-B., Dinsdale, E. A., Willis, B. L., & Bourne, D. G. (2010). Do the organic
 1394 sulfur compounds DMSP and DMS drive coral microbial associations? *Trends in*
 1395 *Microbiology*, *18*, 101–108. <https://doi.org/10.1016/j.tim.2009.12.002>
- 1396 Raina, J.-B., Tapiolas, D. M., Forêt, S., Lutz, A., Abrego, D., Ceh, J., et al. (2013).
 1397 DMSP biosynthesis by an animal and its role in coral thermal stress response.
 1398 *Nature*, *502*, 677–680. <https://doi.org/10.1038/nature12677>
- 1399 Ramakrishnan, S., & Wayne, N. L. (2008). Impact of bisphenol-a on early embryonic
 1400 development and reproductive maturation. *Reproductive Toxicology (Elmsford,*
 1401 *N.Y.)*, *25*, 177–183. <https://doi.org/10.1016/j.reprotox.2007.11.002>
- 1402 Reaka-Kudla, M. L. (1997). The global biodiversity of coral reefs: A comparison
 1403 with rainforests. In Marjorie L. Reaka-Kudla, Don E. Wilson, and Edward O.
 1404 Wilson (Ed.), *Biodiversity II: Understanding and protecting our biological resources*
 1405 (pp. 83–108). Washington, D.C., DC: National Academies Press. Retrieved from
 1406 <https://www.researchgate.net/publication/239063261>
- 1407 Reisch, C. R., Moran, M. A., & Whitman, W. B. (2011). Bacterial catabolism
 1408 of dimethylsulfoniopropionate (DMSP). *Frontiers in Microbiology*, *2*, 172.
 1409 <https://doi.org/10.3389/fmicb.2011.00172>
- 1410 Rendell-Bhatti, F., Paganos, P., Pouch, A., Mitchell, C., D’Aniello, S., Godley, B.
 1411 J., et al. (2021). Developmental toxicity of plastic leachates on the sea urchin
 1412 paracentrotus lividus. *Environmental Pollution (Barking, Essex: 1987)*, *269*,
 1413 115744. <https://doi.org/10.1016/j.envpol.2020.115744>
- 1414 Richmond, R. H. (1997). Reproduction and recruitment in corals: Critical links in the
 1415 persistence of reefs. In *Life and death of coral reefs* (pp. 175–197). Boston, MA:
 1416 Springer US. https://doi.org/10.1007/978-1-4615-5995-5_8
- 1417 Richmond, R. H., Tisthammer, K. H., & Spies, N. P. (2018). The effects of an-
 1418 thropogenic stressors on reproduction and recruitment of corals and reef or-
 1419 ganisms. *Frontiers in Marine Science*, *5*, 379626. [https://doi.org/10.3389/](https://doi.org/10.3389/fmars.2018.00226)
 1420 [fmars.2018.00226](https://doi.org/10.3389/fmars.2018.00226)

- 1421 Ritchie, H. (2026, May 18). Share of global plastic waste emitted to the ocean. Re-
 1422 trieved May 20, 2026, from <https://ourworldindata.org/grapher/share-of>
 1423 [-global-plastic-waste-emitted-to-the-ocean](https://ourworldindata.org/grapher/share-of-global-plastic-waste-emitted-to-the-ocean)
- 1424 Rochman, C. M., Brookson, C., Bikker, J., Djuric, N., Earn, A., Bucci, K., et al.
 1425 (2019). Rethinking microplastics as a diverse contaminant suite. *Environmental*
 1426 *Toxicology and Chemistry*, *38*, 703–711. <https://doi.org/10.1002/etc.4371>
- 1427 Saliu, F., Montano, S., Lasagni, M., & Galli, P. (2020). Biocompatible solid-phase
 1428 microextraction coupled to liquid chromatography triple quadrupole mass
 1429 spectrometry analysis for the determination of phthalates in marine inverte-
 1430 brate. *Journal of Chromatography A*, *1618*, 460852. [https://doi.org/10.1016/](https://doi.org/10.1016/j.chroma.2020.460852)
 1431 [j.chroma.2020.460852](https://doi.org/10.1016/j.chroma.2020.460852)
- 1432 Slattery, M., Hines, G. A., Starmer, J., & Paul, V. J. (1999). Chemical signals in ga-
 1433 metogenesis, spawning, and larval settlement and defense of the soft coral *sinularia*
 1434 *polydactyla*. *Coral Reefs*, *18*, 75–84. <https://doi.org/10.1007/s003380050158>
- 1435 Souter, D., Planes, S., Wicquart, J., Logan, M., Obura, D., & Staub, F. (2020). *Status*
 1436 *of coral reefs of the world: 2020* (research report) (p. 20). UN Environmental
 1437 Programme: Global Coral Reef Monitoring Network & International Coral Reef
 1438 Initiative. Retrieved from [https://gcrmn.net/wp-content/uploads/2021/10/](https://gcrmn.net/wp-content/uploads/2021/10/Executive-Summary-with-Forewords.pdf)
 1439 [Executive-Summary-with-Forewords.pdf](https://gcrmn.net/wp-content/uploads/2021/10/Executive-Summary-with-Forewords.pdf)
- 1440 Stephens, T. G., Lee, J., Jeong, Y., Yoon, H. S., Putnam, H. M., Majerová, E., &
 1441 Bhattacharya, D. (2022). High-quality genome assemblies from key hawaiian coral
 1442 species. *GigaScience*, *11*, giac098. [https://doi.org/10.1093/gigascience/](https://doi.org/10.1093/gigascience/giac098)
 1443 [giac098](https://doi.org/10.1093/gigascience/giac098)
- 1444 Stubbins, A., Law, K. L., Muñoz, S. E., Bianchi, T. S., & Zhu, L. (2021). Plastics
 1445 in the earth system. *Science (New York, N.Y.)*, *373*, 51–55. [https://doi.org/](https://doi.org/10.1126/science.abb0354)
 1446 [10.1126/science.abb0354](https://doi.org/10.1126/science.abb0354)
- 1447 Tarrant, A. M. (2005). Endocrine-like signaling in cnidarians: Current understanding
 1448 and implications for ecophysiology. *Integrative and Comparative Biology*, *45*,
 1449 201–214. <https://doi.org/10.1093/icb/45.1.201>
- 1450 Tarrant, Ann M. (2007). Hormonal signaling in cnidarians: Do we understand the
 1451 pathways well enough to know whether they are being disrupted? *Ecotoxicology*
 1452 *(London, England)*, *16*, 5–13. <https://doi.org/10.1007/s10646-006-0121-1>
- 1453 Tarrant, A. M., Atkinson, S., & Atkinson, M. J. (1999). Estrone and estradiol-17 beta
 1454 concentration in tissue of the scleractinian coral, *montipora verrucosa*. *Comparative*
 1455 *Biochemistry and Physiology. Part A, Molecular & Integrative Physiology*, *122*,
 1456 85–92. [https://doi.org/10.1016/s1095-6433\(98\)10155-1](https://doi.org/10.1016/s1095-6433(98)10155-1)
- 1457 Tarrant, Ann M., Blomquist, C. H., Lima, P. H., Atkinson, M. J., & Atkinson, S.
 1458 (2003). Metabolism of estrogens and androgens by scleractinian corals. *Comparative*
 1459 *Biochemistry and Physiology. Part B, Biochemistry & Molecular Biology*, *136*,
 1460 473–485. [https://doi.org/10.1016/s1096-4959\(03\)00253-7](https://doi.org/10.1016/s1096-4959(03)00253-7)
- 1461 Tarrant, A. M., Atkinson, M. J., & Atkinson, S. (2004). Effects of steroidal estrogens
 1462 on coral growth and reproduction. *Marine Ecology Progress Series*, *269*, 121–129.
 1463 <https://doi.org/10.3354/meps269121>
- 1464 Tetu, S. G., Sarker, I., Schrameyer, V., Pickford, R., Elbourne, L. D. H., Moore, L. R.,
 1465 & Paulsen, I. T. (2019). Plastic leachates impair growth and oxygen production in
 1466 prochlorococcus, the ocean’s most abundant photosynthetic bacteria. *Communica-*
 1467 *tions Biology*, *2*, 184. <https://doi.org/10.1038/s42003-019-0410-x>
- 1468 Thiel, D., Yañez-Guerra, L. A., Kieswetter, A., Cole, A., Temmerman, L., Technau,
 1469 U., & Jékely, G. (2023). Large-scale deorphanization of *nematostella vectensis*
 1470 neuropeptide GPCRs supports the independent expansion of bilaterian and
 1471 cnidarian peptidergic systems. *bioRxiv*, 2023.07.03.547448. [https://doi.org/](https://doi.org/10.1101/2023.07.03.547448)
 1472 [10.1101/2023.07.03.547448](https://doi.org/10.1101/2023.07.03.547448)
- 1473 Twan, W.-H., Hwang, J.-S., Lee, Y.-H., Wu, H.-F., Tung, Y.-H., & Chang, C.-F.
 1474 (2006). Hormones and reproduction in scleractinian corals. *Comparative Biochem-*

- 1475 *istry and Physiology. Part A, Molecular & Integrative Physiology, 144*, 247–253.
 1476 <https://doi.org/10.1016/j.cbpa.2006.01.011>
- 1477 Vandenberg, L. N. (2021). Endocrine disrupting chemicals: Strategies to protect
 1478 present and future generations. *Expert Review of Endocrinology & Metabolism, 16*,
 1479 135–146. <https://doi.org/10.1080/17446651.2021.1917991>
- 1480 Vandenberg, L. N., Colborn, T., Hayes, T. B., Heindel, J. J., Jacobs, D. R., Jr,
 1481 Lee, D.-H., et al. (2012). Hormones and endocrine-disrupting chemicals: Low-
 1482 dose effects and nonmonotonic dose responses. *Endocrine Reviews, 33*, 378–455.
 1483 <https://doi.org/10.1210/er.2011-1050>
- 1484 Vega Thurber, R., Willner-Hall, D., Rodriguez-Mueller, B., Desnues, C., Edwards,
 1485 R. A., Angly, F., et al. (2009). Metagenomic analysis of stressed coral holo-
 1486 bionts. *Environmental Microbiology, 11*, 2148–2163. <https://doi.org/10.1111/j.1462-2920.2009.01935.x>
- 1487 Vered, G., & Shenkar, N. (2022). Limited effects of environmentally-relevant concen-
 1488 trations in seawater of dibutyl phthalate, dimethyl phthalate, bisphenol a, and
 1489 4-nonylphenol on the reproductive products of coral-reef organisms. *Environmental*
 1490 *Pollution (Barking, Essex: 1987), 314*, 120285. <https://doi.org/10.1016/j.envpol.2022.120285>
- 1491 Vilella, H., Modolon, F., Schultz, J., Delgadillo-Ordoñez, N., Carvalho, S., Sori-
 1492 ano, A. U., & Peixoto, R. S. (2023). Genome analysis of a coral-associated
 1493 bacterial consortium highlights complementary hydrocarbon degradation abil-
 1494 ity and other beneficial mechanisms for the host. *Scientific Reports, 13*, 12273.
 1495 <https://doi.org/10.1038/s41598-023-38512-z>
- 1496 Vlaanderen, E., Ghaly, T., Moore, L., Focardi, A., Paulsen, I., & Tetu, S. (2023).
 1497 Plastic leachate exposure drives antibiotic resistance and virulence in marine
 1498 bacterial communities. *bioRxiv*, 2023.02.13.528379. <https://doi.org/10.1101/2023.02.13.528379>
- 1499 Wang, Y., Naumann, U., Wright, S. T., & Warton, D. I. (2012). Mvabund— an R
 1500 package for model-based analysis of multivariate abundance data: The mvabund
 1501 R package. *Methods in Ecology and Evolution, 3*, 471–474. <https://doi.org/10.1111/j.2041-210x.2012.00190.x>
- 1502 Weis, J. S., & Palmquist, K. H. (2021). Reality check: Experimental studies on
 1503 microplastics lack realism. *Applied Sciences (Basel, Switzerland), 11*, 8529.
 1504 <https://doi.org/10.3390/app11188529>
- 1505 Wickham, H., Averick, M., Bryan, J., Chang, W., McGowan, L., François, R., et
 1506 al. (2019). Welcome to the tidyverse. *Journal of Open Source Software, 4*, 1686.
 1507 <https://doi.org/10.21105/joss.01686>
- 1508 Wilkins, K. W., & Richmond, R. H. (2025). Unseen threats: Negative effects of
 1509 microplastic leachate on coral planulae settlement. *Frontiers in Marine Science, 12*,
 1510 1596594. <https://doi.org/10.3389/fmars.2025.1596594>
- 1511 Wilkins, K. W., Yew, J. Y., Seeley, M., & Richmond, R. H. (2024). Microplastic
 1512 leachate negatively affects fertilization in the coral *montipora capitata*. *Integrative*
 1513 *and Comparative Biology, 64*, 1131–1140. <https://doi.org/10.1093/icb/icae143>
- 1514 Woolsey, E. S., Byrne, M., & Baird, A. H. (2013). The effects of temperature on
 1515 embryonic development and larval survival in two scleractinian corals. *Marine*
 1516 *Ecology Progress Series, 493*, 179–184. <https://doi.org/10.3354/meps10499>
- 1517 Xu, H., Cao, W., Sun, H., Zhang, S., Li, P., Jiang, S., & Zhong, C. (2021). Dose-
 1518 dependent effects of di-(2-ethylhexyl) phthalate (DEHP) in mussel *mytilus*
 1519 *galloprovincialis*. *Frontiers in Marine Science, 8*, 658361. <https://doi.org/10.3389/fmars.2021.658361>
- 1520 Zhang, Y., Jiao, Y., Li, Z., Tao, Y., & Yang, Y. (2021). Hazards of phthalates
 1521 (PAEs) exposure: A review of aquatic animal toxicology studies. *The Sci-*
 1522 *ence of the Total Environment, 771*, 145418. <https://doi.org/10.1016/j.scitotenv.2021.145418>